tructure-Function Analysis of the EsaR N-terminal Domain

Jared S. Geissinger

Dissertation submitted to the faculty of the Virginia Polytechnic Institute and State University in partial fulfillment of the requirements for the degree of

Master of Science
in
Biological Sciences

Ann M. Stevens, Committee Chair
Florian D. Schubot
David L. Popham
Marcy Hernick

November 17, 2011

Blacksburg, VA

Keywords: EsaR, LuxR homologue, *Pantoea stewartii*, quorum sensing, transcriptional repressor

Structure-Function Analysis of the EsaR N-terminal Domain

Abstract

The LuxR protein family is a class of quorum-sensing regulated bacterial transcription factors that alter gene expression as a function of ligand detection. This coincides with a high population density and/or a low rate of signal ligand diffusion. The majority of LuxR proteins are activated only in the presence of the signal ligand, an acyl-homoserine lactone (AHL). EsaR, from the corn pathogen *Pantoea stewartii*, represents a subset of LuxR homologues that are active in the absence of AHL and deactivated by its presence. The mechanism by which EsaR responds to AHL in a manner opposite to that of the majority of LuxR homologues remains elusive. Unlike the majority of LuxR homologues, which require AHL for purification, EsaR can be purified and biochemically investigated in the absence and presence of AHL. This work sought to answer questions regarding the structure-function relationship of the LuxR homologue, EsaR.

Fluorescence anisotropy was used to determine the relative DNA-binding affinity of wild type EsaR and three AHL-independent EsaR variants in the presence and absence of AHL. This enabled for quantitative analysis of the relative binding affinities of these AHL-independent variants for the EsaR binding site, the *esa* box. The results demonstrate that one AHL-independent EsaR variant has a slightly higher affinity for the *esa* box in the presence, rather than the absence of AHL. The affinity of the other two for the DNA is not impacted by AHL, potentially due to an inability to transduce the signal of ligand detection to the DNA binding domain.

Constructs containing only the EsaR N-terminal domain (NTD) were also developed. These constructs circumvented solubility issues associated with the full-length protein, allowing for additional

biochemical analysis. It was determined that the EsaR NTD alone is sufficient for multimerization and ligand binding. Additionally, preliminary X-ray crystallography efforts have established some of the early parameters required to solve the crystal structure of the EsaR ligand binding domain in both the presence and absence of AHL. If pursued, these structures would be the first solved of a LuxR homologue ligand binding domain in both the presence and absence of the native AHL, potentially demonstrating the conformational change that occurs as a result of ligand binding. Collectively, these findings have established some of the groundwork required to resolve the question of what sort of conformational changes occur in EsaR as a result of ligand binding.

Acknowledgements

It goes without saying that the greatest acknowledgement that I have to give goes to Ann. You took a major risk accepting me into your lab and I hope that in retrospect you conclude that it was a good decision. For all of the gray hairs that I may have caused, I am sorry. I hope that you will know that I am greatly thankful for all of your support, guidance, patience and cooperation that you have given me.

Dr. Schubot, you have been great source of knowledge and wisdom in regards to research and life in general. For all of the time that you have invested into me, answering the many questions that I had, I am grateful. If I ever needed advice or criticism, I always knew where I could turn to. Though sometimes annoying, I know that the criticism that I received from you was invaluable in molding the way I interpret data and conduct experiments.

Dr. Popham, thank you for your excellent suggestions and criticisms given regarding my research, particularly in the direction of controls. Your feedback has become an integral part of the way I conduct experiments. Thanks to the suggestions that you have given, I have a much better understanding of the importance of controls and how to incorporate them.

Dr. Hernick, thank you for laying the initial groundwork from which my graduate studies advanced. You provided me with my first major opportunity of conducting bench work. While I didn't entirely understand the work that I performed in your lab in my earliest days of graduate school, the principles indubitably helped me further down the road. You have been a great source of knowledge for questions regarding biochemistry, especially fluorescence anisotropy.

Dr. Black, thank you for your random nuggets of knowledge. The accessibility of a next door researching scientist has proven invaluable. Even though you have no vested role in this project, I always knew that I could turn to you for trouble-shooting advice. Your reputation of the Life Sciences 1 Allah is well deserved. Good luck raising chickens (and maybe expanding the farming interest).

Revathy (aka pre-lim), Alison and Regina, it has been fun "enjoying" Q99, West End cookies and chocolate (outside of the lab of course). For all of the lab memories that I do and don't recall, it has been fun (at least mostly). Good luck with wherever you go and whatever you decide to do.

Cory Bernhards, thank you for being a source of commiseration regarding fluorescence anisotropy. I now have a better understanding of the pain that this assay has put you through. It has also been fun enjoying lunch together almost daily (you too, Casey). It has also been fun playing softball.

Dr. Scharf and lab, thank you for being an excellent source of socialization and purchasing of free-range chicken eggs.

Lastly I'd like to thank my family, especially my parents, for all of the support of many varieties over the years, not limited to graduate school. I am thankful to know that I have a continual source of support and encouragement that I can turn to in any situation.

Table of Contents

List of Figures

Page number

List of Tables

Page number

Chapter I

Literature Review

Quorum sensing

Once considered to be organisms concerned with only their own propagation, many bacteria are now known to coordinate group behaviors utilizing a form of communication known as quorum sensing (QS). Using QS, both Gram-positive and Gram-negative bacteria are able to function in unison to achieve coordination of multicellular processes that would be futile if performed by an individual cell. Bacterial processes controlled by QS include conjugation, bioluminescence, biofilm maturation, antibiotic production, and expression of an array of virulence factors (27, 30, 88, 91).

QS in both Gram-positive and Gram-negative bacteria generally relies on two major components; a chemical signal and a cognate transcription factor. The chemical signal is a low weight compound referred to as an autoinducer (AI) and its concentration increases with population density. At high concentrations, the AI is detected by a cognate transcription factor. The transcription factor is then responsible for AI-dependent regulation of genes, either up-regulating or down-regulating expression.

Although QS is found across the bacterial domain, there are fundamental differences in the Q-S systems of different bacteria. The AI primarily used by Gram-positive bacteria is typically a short peptide which is detected by membrane-spanning kinases (20). The AI commonly used by Gram-negative proteobacteria is a diffusible acyl-homoserine lactone (AHL) which increases in concentration with population density. In some organisms, AHL production is linear whereas other organisms utilize a positive feedback loop in which AHL expression upregulates itself (92).

At a critical threshold concentration, the AHL diffuses across the cell membrane and into the bacterial cell where it is detected by its cognate transcription factor (30, 88).

Traditionally QS was thought to serve as a means for intra-species communication. However, additional Q-S signals have been discovered and are believed to serve as a means of inter-species communication (58, 88). Generically termed AI-2, these signals are thought to have implications for flora development and control. *Vibrio harveyi* was the first organism found to utilize a furanosyl borate diester AI-2 signal (13).Furthermore, recent studies suggest that QS may be used as a mechanism of inter-kingdom signaling and may have implications for bacteria-plant and bacteria-human relationships (38). Though the majority of bacterial Q-S systems involve the use of peptides and AHL, exceptions have since been discovered in Gram-positive and Gram-negative bacteria alike (13, 46, 66). For example, *Bradyrhizobium japonicum* uses bradyoxetin for QS (46) and various species of Gram-negative bacteria have been found to use cyclic dipeptides (37).

Due to the metabolic demands of QS, social "cheaters" have arisen. "Cheaters" reap the benefit of the group behavior while lacking their own contribution, typically due to the loss of Q-S controlled transcription factors (25, 65, 84). Interestingly, pathogenic social cheaters, such as *Pseudomonas aeruginosa*, lose virulence after multiple generations (65). Exploitation of this social cheating is one of several examples of how an understanding of QS could be used for medical applications, particularly in regards to virulence.

Medical implications of quorum sensing

Since its discovery in the 1970s, QS has been found to be a widespread phenomenon. *Pseudomonas aeruginosa*, notorious for causing nosocomial infections and its association with cystic fibrosis, has served as a model system for QS due to its clinical relevance (27). Ideally, QS used by pathogens could be controlled to interfere with the production or activity of associated virulence factors via a method commonly referred to as quorum quenching (19). The primary focus of quorum quenching has been the synthesis of AI homologues that cause the cognate receptor to lock into an unresponsive state. Recent work is now focused on identifying compounds that not only inhibit AI production but also act upon the cognate AI receptor (16). Environmental examples of quorum quenching do exist and could be exploited for use in a clinical setting (75). Additionally, advances in synthetic biology have devised a system in which population density can be controlled via programed death utilizing a Q-S circuit (95). Organisms that utilize QS could potentially be exploited to neutralize their vector host, holding implications for prevention of diseases such as malaria (5).

Early studies on quorum sensing

Vibrio fischeri first caught the interest of investigators for its ability to colonize the Japanese pinecone fish, *Monocentris japonicus*, where it induces the production of bioluminescence. It has subsequently been found to inhabit the Hawaiian bobtailed squid, *Euprymna scolopes* (89). Here the bacteria, when living in association with the host, also provide bioluminescence. The light serves for counter-illumination, a defense mechanism for the squid which removes a shadow that could otherwise be cast and detected by predators. In exchange for light

production, the bacteria are provided with a stable environment and an ample supply of nutrients (29, 64).

Studies on QS in *V. fischeri* (formerly *Photobacterium fischeri*) initiated in the 1970s (41, 57). It was initially thought that the culture medium contained a luminescence inhibition substance that was degraded by bacteria as the population density increased. Medium in which bacteria grew and displayed luminescence was considered to be "conditioned." When a fresh bacterial culture was introduced into the "conditioned" medium, luminescence was observed almost instantaneously (41). It was later shown that luminescence occurred only when cultures reached the late exponential growth phase. Investigators hypothesized that the bacteria reached a critical concentration at which induction of luciferase ensued, resulting in luminescence. This phenomenon became known as "autoinduction" and was found to be reliant upon an unidentified "autoinducer" (21, 57), later discovered to be an AHL (22). It has subsequently been shown that QS is a widespread process, occurring in a number of bacterial species, with new examples continually being identified.

LuxI and LuxR

Studies in molecular biology have demonstrated that regulation of the luminescence observed in *V. fischeri* is due to a two-part communication mechanism. The first part is an AHL chemical signal. The second part is the LuxR transcription factor which detects the AHL. The transcription factor is then responsible for the up-regulation of several genes, including the *lux* operon.

The AHLs used by Gram-negative proteobacteria have a conserved homoserine lactone ring, but alterations in the acyl chain allow for species-specific detection. The acyl chain can range from four to eighteen carbons (30) and can have other modifications, particularly at the third carbon in the acyl chain. The AHL used by *V. fischeri* is *N*-3-(oxohexanoyl)-L-homoserine lactone (3-oxo-C6-HSL) (22), which is produced by the *luxI* gene product (22-24, 67).

In the presence of high concentrations of its cognate AHL, LuxR activates transcription of the *lux* operon, comprised of *luxICDABEG*. The *lux* operon, required for luminescence, is activated when LuxR binds to a palindromic DNA segment known as the *lux* box, centered at the -42.5 site in the *lux* operon promoter (3, 24, 43, 72). The positioning of the *lux* box allows for LuxR to bind and make interactions with RNA polymerase (RNAP) resulting in activation (18, 26, 40, 78). *luxI* codes for the positively regulated AI synthase (23). The luciferase α and β subunits are encoded by *luxA* and *luxB*, respectively (50). A fatty acid reductase complex is required for synthesis of the aldehyde substrate used by luciferase. Components of this complex are encoded by *luxC*, *luxD* and *luxE* (24). Though not required for luminescence, *luxG* is thought to encode a flavin mononucleotide reductase that generates a reduced flavin mononucleotide that is used by luciferase (3).

It was originally thought that most organisms had only one AHL synthase gene and cognate receptor. However, more recently it has been discovered that some organisms may have multiple Q-S networks. One example exists in *Vibrio fischeri* in which AinS produces a C8-HSL which is detected by AinR (31). The prevalence of a second Q-S network has no obvious

consequence in some organisms while in other organisms, such as *Pseudomonas aeruginosa*, a second Q-S network allows for a regulation hierarchy of genes controlled by QS (61).

V. fischeri has served as the model organism of Q-S investigation, but numerous LuxI and LuxR homologues have been found in an array of other Gram-negative proteobacteria. The focus of this thesis research was on the LuxR homologue, EsaR, found in the corn pathogen, *Pantoea stewartii*, ssp. *stewartii*.

Pantoea stewartii

Pantoea stewartii ssp. *stewartii* (*P. stewartii*, formerly *Erwinia stewartii*) is the causative agent of Stewart's wilt disease in sweet corn and leaf blight in maize (43, 51) (for review see (63)). Initially thought to be a non-motile, non-sporulating, Gram-negative bacillus with similarities to *Escherichia coli* (*E. coli*), it has since been determined to be capable of surface motility dependent upon the production of exopolysaccharide (EPS) (7, 36).

Corn can become infected with *P. stewartii* via contaminated soil or manure, but the most common mode of infection is via the corn flea beetle, *Chaetocnema pulicaria*. Because the incidence of infection is primarily determined by beetle population levels, higher temperatures and mild winters, coinciding with increased beetle survival, are predictive of a season of high infection incidence (17).

The major virulence factor of *P. stewartii* is Stewartan, an EPS exhibited as a yellow, slimy extrusion from the cut stems of maize (*Zea mays*) infected by the bacterium. It is a repeating heptasaccharide composed of glucose, galactose and glucuronic acid in a 3:3:1 ratio,

respectively (59). This EPS blocks plant host defenses and causes necrotic lesions via vascular flow obstruction (8).

It is not the mere production of EPS that causes Stewart's wilt disease, but rather the temporal timing of expression of genes involved in this Q-S regulated network. Initial stages of infection occur when a *hrp* (hypersensitive response and pathogenicity) type-III secretion system deploys *wts* (water soaking) effector proteins which induce electrolyte leakage and tissue water soaking (1, 87). This early stage of infection allows the bacteria to overcome host defenses and disseminate from the intercellular space. The bacteria then preferentially colonize the xylem, building in cell density. Once a critical cell density is reached (~$2x10^8$ cells/ml; AHL concentration of 2 μM) (86), the Q-S virulence cascade is activated. An unidentified environmental signal stimulates RcsF, an outer membrane lipoprotein which serves as an alternate sensor-kinase for RcsB (49). RcsF transmits the signal to the membrane bound sensor-kinase, RcsC. RcsC then transmits the phosphoryl group to an intermediate membrane-associated protein, RcsD. RcsD transmits the phosphoryl group to the cytoplasmic response regulator, RcsB. Upon receiving the signal, RcsB undergoes a conformational change which allows it to form a heterodimer with another response regulator, RcsA. Once bound by AHL, EsaR dissociates from the *esa* box, a 20 bp palindromic DNA sequence at the promoters of *rcsA* and *esaR*. This dissociation allows for the transcription of *rcsA* (4, 86) (Figure 1.1). The RcsAB heterodimer binds to the promoter of the *cps* operon, resulting in the production of EPS (9, 48, 77, 87).

EsaI and EsaR control of gene expression in *P. stewartii*

EsaI and EsaR are LuxI and LuxR homologues that use QS to coordinate the production of EPS, the major virulence factor in *P. stewartii* (4). In the absence of AHL, coinciding with a low population density, EsaR binds to the *esa* box. Centered at the -10 site, the positioning of the *esa* box, when bound by dimeric EsaR, prevents RNA polymerase (RNAP) from transcribing the *rcsA* regulatory gene required to induce EPS synthesis (9, 52, 53).

EsaI is the LuxI homologue that primarily produces 3-oxo-C6-HSL, the same AHL used by *Vibrio fischeri* (4). Although this is the major product of EsaI that EsaR responds to, subnanomolar concentrations of *N*-3-oxo-octanoyl-HSL, the AHL used by TraR (39), have also been detected as an EsaI product (86). Unlike other LuxI homologues which are commonly autoregulated, EsaI is constitutively expressed and expression is independent of EsaR (53). Furthermore, *esaI* is unique in the respect that it is convergently transcribed from *esaR* and these transcripts have an overlapping region of ~30 bases. This is atypical for LuxI and LuxR homologues as most are divergently transcribed (4, 86).

Initially classified as the first LuxR homologue to function as a repressor of transcription, EsaR has since been determined to also serve as an activator (69, 85, 86). Studies using recombinant *E. coli* have demonstrated that in the absence of AHL, EsaR can activate the *lux* operon (85). This activation only occurs in the absence of AHL and activity is abolished in its presence (85). When the *esa* box is centered at -42.5 on the promoter, EsaR is capable of functioning as an activator (69). In its native host, *P. stewartii*, EsaR is capable of activating expression of a sRNA in the absence of AHL (69). Similar to EsaR, LasR from *Pseudomonas aeruginosa* has been

shown to bind to the *lux* box And LuxR is capable of binding to the *esa* box (85) and the *las* box (33). These data suggest that there is conserved functionality in the DNA binding capability of these proteins and that it is the position of the *esa* box that controls whether EsaR functions as an activator or a repressor.

The LuxR protein family

LuxR homologues share a similar structure in that they are comprised of an N-terminal domain (NTD) and a C-terminal domain (CTD). The NTD binds to AHL whereas the CTD binds to DNA (14, 15, 35) (Figure 1.2). However, the mechanism by which any member of this family changes its conformation in response to the binding of a native AHL remains to be determined.

The LuxR protein family is composed of five classes of homologous transcription factors (74) (Figure 1.3). The first three classes are similar in the respect that they are considered to be "activators," transcription factors that require AHL to recruit RNAP to activate transcription of genes controlled by QS. Class one members have a co-translational requirement for their cognate AHL and display binding that is virtually irreversible (99). When translated in the absence of their cognate AHL, these proteins are unstable and subject to proteolysis, primarily by Clp and Lon proteases (100). An example of a class one member is TraR from *Agrobacterium tumefacians.* Class two members do not have a co-translational requirement for AHL, but protein stability is enhanced by its presence. Unlike class one members, AHL binding is reversible for class two members. LuxR is the best studied class two member (81). The third class encompasses LuxR homologues that do not require AHL for enhanced stability or proper folding, but AHL is required for dimerization and activation. MrtR from *Mesorhizobium*

tianshanense is an example of a class three member (98). In contrast to classes one through three, class four members bind to DNA as a dimer in the absence of AHL, preventing RNAP from transcribing genes under the control of QS while activating expression of others, contingent upon the position of the binding site. In the presence of AHL, class four members dissociate from DNA, allowing for RNAP to transcribe the genes that were otherwise repressed or deactivating genes that were activated in the presence of AHL. Gel filtration and crosslinking assays have suggested that the multimeric state of class four members does not change in the presence or absence of AHL (70). Additionally, in comparison to other LuxR proteins they are relatively stable in the absence of AHL. Pulse-chase experiments have demonstrated that EsaR, a class four member, does not display differential susceptibility to proteolysis in the presence versus the absence of AHL (70). These members have two unique regions in comparison to members of other classes; they have an extended linker region connecting the NTD and the CTD and they also have an extended CTD (Figure 1.2). EsaR was the first class four member discovered and has been the most extensively investigated (4, 60, 74).Many of these LuxR homologues autorepress their own synthesis in the absence of AHL (10, 52). Finally, class five members are considered to be “orphan” LuxR homologues as they do not have a related LuxI homologue. The AHLs sequestered by these members are produced by neighboring bacteria. Class five members remain monomeric in the presence and absence of AHL. SdiA from *E. coli* is an example of a class five homologue (94).

EsaR represents a subset of LuxR homologues that serve as repressors of transcription in the absence of AHL and are deactivated when bound to AHL. Because EsaR was the first example of

a repressor identified, it has been subject to extensive biochemical analysis. More examples of repressors have since been discovered, with examples including ExpR of *Erwinia carotovorum* (2), ExpR of *Erwinia chrysanthemi* (56), SmaR of *Serratia* sp. ATCC 39006 (76), EanR of *Pantoea ananatis* (54), and YenR of *Yersinia enterocolitica* (80). Aside from their response to AHL, these regulators are also similar in the sense that the genes encoding them are convergently transcribed from their cognate AHL synthase genes.

The mechanism by which EsaR responds to AHL in a manner opposite to that of the majority of LuxR homologues remains an unresolved question in the Q-S field. Because EsaR is functional in the absence of AHL, unlike the majority of LuxR proteins, it is well suited for biochemical analysis in the presence and absence of AHL. The work presented herein demonstrates that amino acid substitutions in the EsaR NTD impact interdomain signaling to the CTD (Chapter 2). Additionally this work shows that the presence of AHL does not impact the multimeric state of EsaR and that the NTD is sufficient for ligand binding and multimerization (Chapter 3). Removal of the CTD has led to improved protein solubility allowing for structural analysis. Structural studies are underway to elucidate the conformational changes that occur in the NTD as a result of AHL binding (Chapter 3).

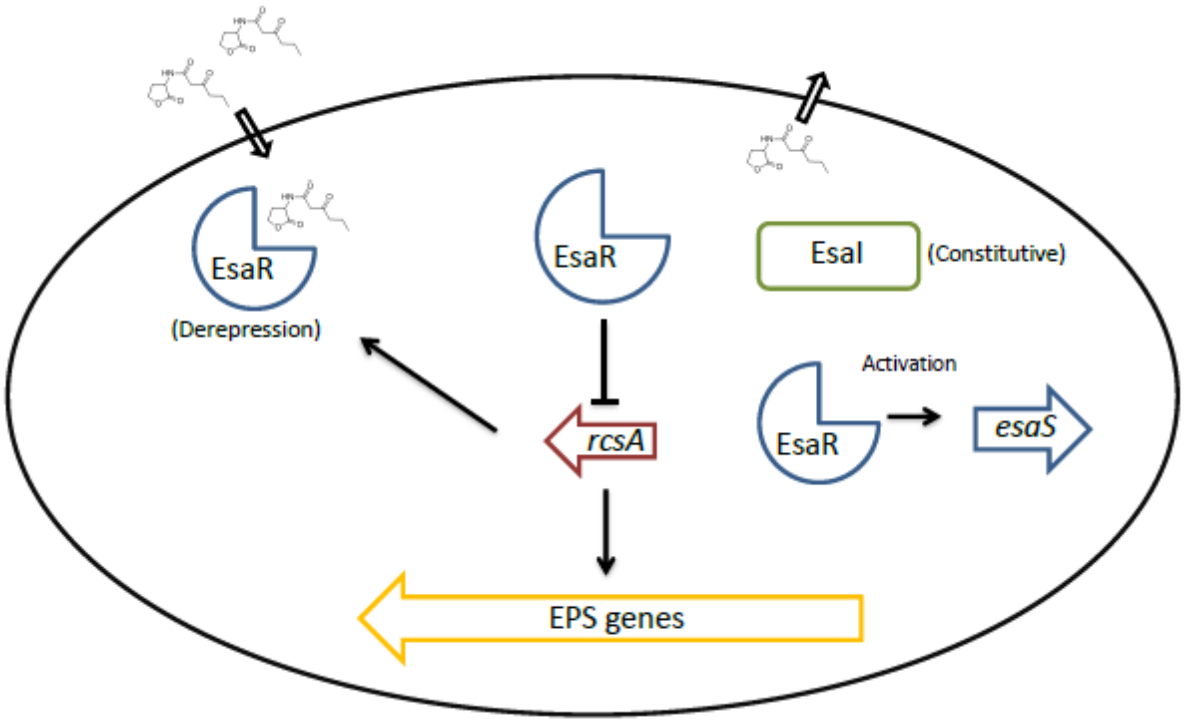

Figure 1.1: Simplified schematic of the quorum-sensing network of *P. stewartii* with an emphasis on EsaR regulation. See the text for details.

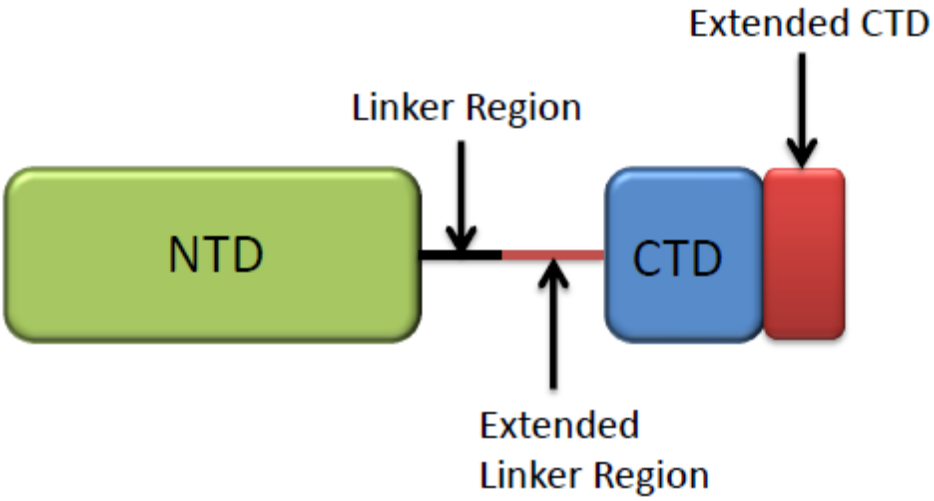

Figure 1.2. Cartoon depiction of the general structure of LuxR homologues. The N-terminal domain (NTD) binds AHL and is connected to the DNA-binding C-terminal domain (CTD) by a linker region. The EsaR subfamily of LuxR homologues contain additional residues in the linker region as well as an extended CTD.

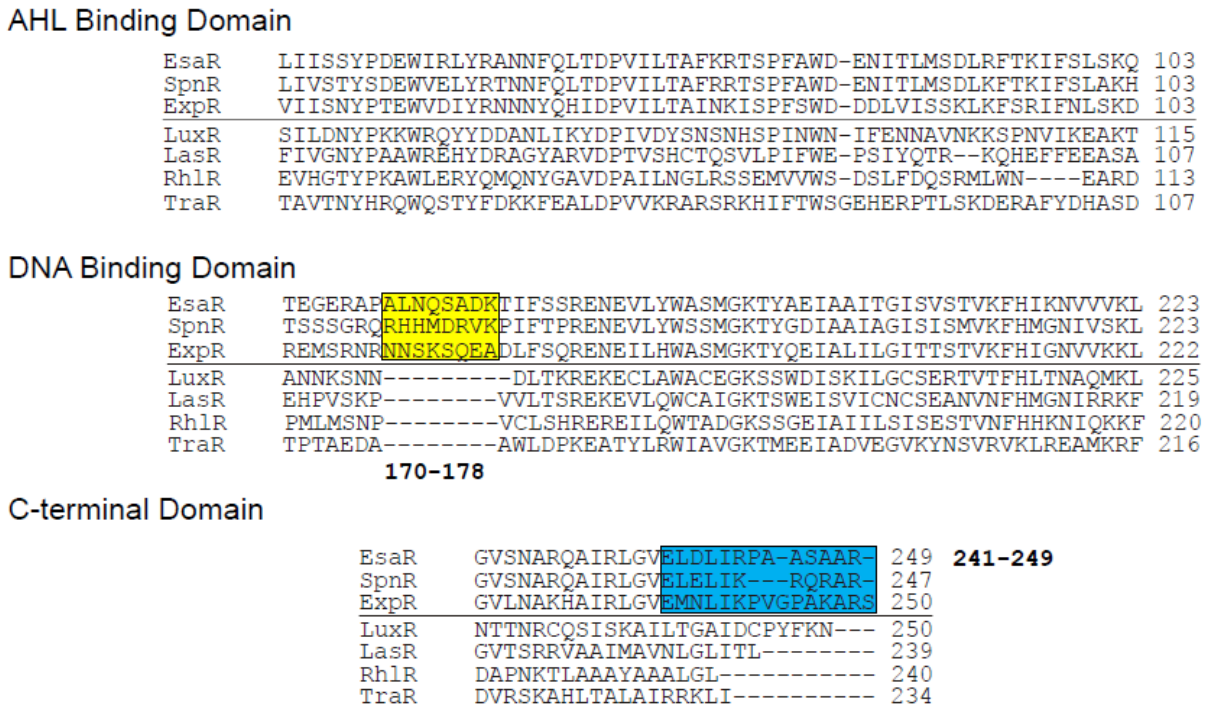

Figure 1.3. ClustalW sequence alignment of LuxR homologues. A ClustalW sequence alignment was modified from (74). Highlighting indicates regions unique to the EsaR subset (EsaR, SpnR, ExpR) of LuxR homologues. Yellow highlighting indicates extended residues in the linker region, blue highlighting indicates extended residues in the C-terminal domain.

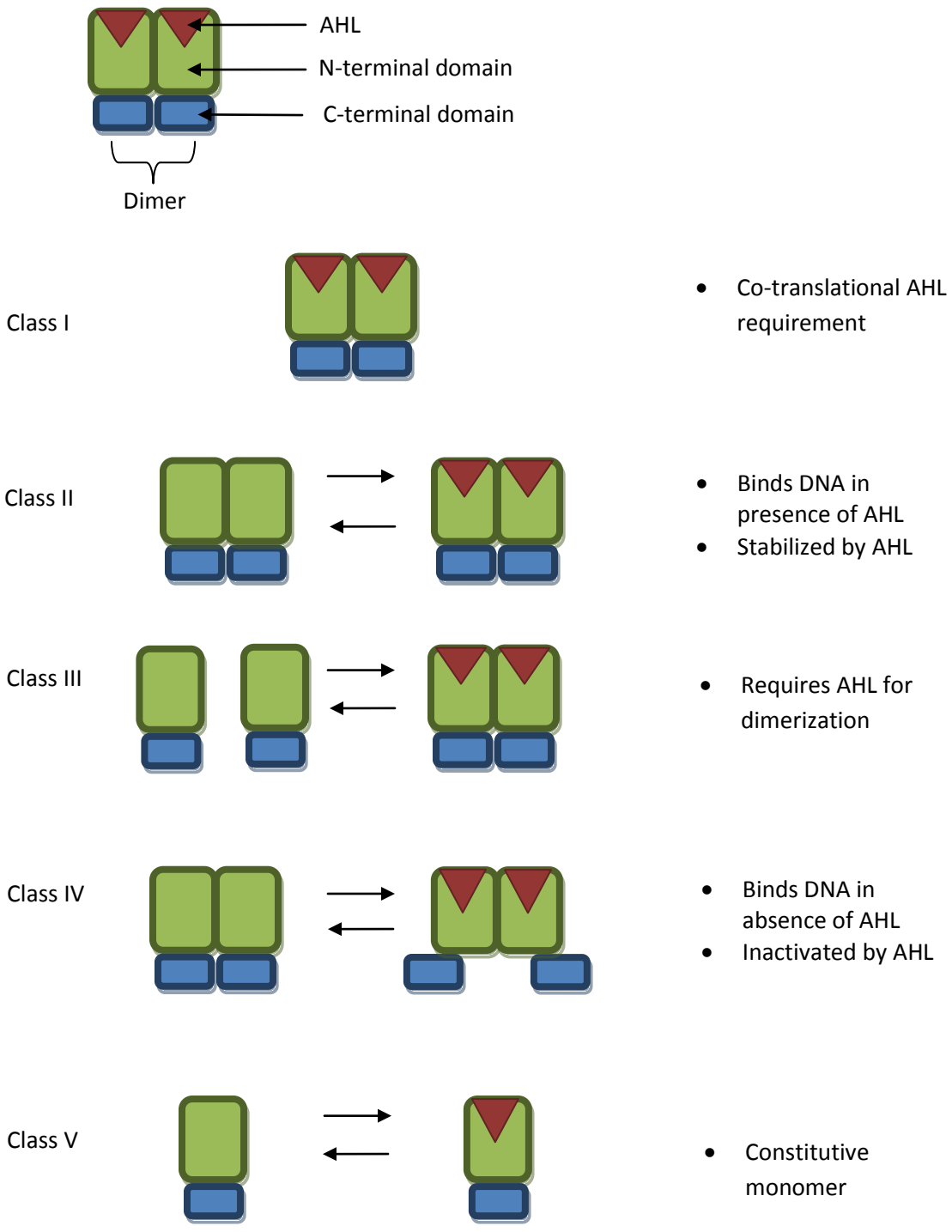

Figure 1.4. The five classes of LuxR homologues. Unique features of each class are listed to the right. With the exception of class IV, all classes are incapable of binding DNA in the absence of AHL, and are capable of binding DNA in the presence of AHL. See text for further details.

Chapter II

Analysis of the Relative DNA Binding Affinities of Select EsaR* Variants

Abstract:

The mechanism by which acyl-homoserine lactone (AHL) causes EsaR to become incapable of binding DNA remains elusive. Random and site-directed mutagenesis of EsaR was previously performed in an attempt to identify residues that are involved with AHL recognition and response. These studies identified eight residues that render EsaR unresponsive to AHL; six are unable to bind AHL, two retain AHL-binding capability but remain unresponsive to it. In this study, fluorescence anisotropy was used to examine the relative DNA binding affinity of two of these EsaR* variants, D83E and F94Y, versus a wild-type control. The results for variants D83E and F94Y suggest that the functionality of the EsaR N-terminal domain is uncoupled from that of the C-terminal domain.

Introduction:

The LuxR protein family represents a class of bacterial transcription factors that alter gene expression in response to ligand detection as a function of the bacterial population density. The ligand detected by LuxR proteins is an acyl-homoserine lactone (AHL), a species-specific chemical signal produced by certain species of bacteria which is sensed by the bacterial population only at a high cell density. To date, only three full-length LuxR homologue structures have been solved (11, 12, 45, 83, 96) while additional structures of ligand-binding domains are also available (6, 94). The majority of solved structures are only available in the presence of the cognate AHL. Given the lack of structural information available as well as the relatively low sequence similarity of LuxR proteins (73), it is difficult to predict which EsaR residues are responsible for AHL recognition and response. This is especially true for the EsaR subfamily, which responds to AHL in a manner opposite to that of the larger LuxR family. In an attempt to identify

residues important for AHL responsiveness in EsaR, error-prone PCR and blue/white β-galactosidase screening assays were previously performed (42).

Error-prone PCR generated 14 EsaR variants that were shown to be unresponsive to AHL (EsaR* variants), as demonstrated through blue/white screening and quantitative β-galactosidase assays. After analyzing sequencing data, it was noted that several variants had multiple mutated residues per construct. To determine the AHL response of individual residues, site-directed mutagenesis was performed to incorporate only one amino acid substitution per construct. This resulted in 25 constructs, 5 of which had a given residue changed into >1 alternate amino acid (32, 74, 101, 104, 243). These constructs were again subjected to quantitative β-galactosidase assays to confirm an AHL-independent phenotype. Results from these assays indicated that alterations of eight residues could contribute to the AHL-independent phenotype (A32V, A81T, D83E, F94Y, F98Y, S101P/S101Y, Y104D/Y104F/Y104N, I106F).

To decipher whether AHL-independent variants were incapable of binding AHL, or if they were unresponsive due to another mechanism, *in vitro* studies were performed. Variants were fused to a His_6-MBP tag in an attempt to circumvent associated solubility issues, creating protein constructs similar to HMGE (70). Purified $EsaR^*$ variants were incubated with AHL. Protein was re-purified to remove unbound AHL. Ethyl acetate was subsequently used to extract AHL bound to the protein. The resulting solution was incubated with an *E. coli* strain harboring a plasmid encoding P_{luxI}-gfp divergently transcribed from *luxR* (85). Because LuxR requires AHL for activation, extracts containing AHL activated *gfp* expression (68).

Six variants were shown to be unresponsive to AHL due to their inability to bind the ligand (A32V, A81T, F98Y, S101P, Y104D, I106F). However, two (D83E, F94Y) retained AHL binding capability, but were

unresponsive to it. Possible explanations for this phenotype are that the mutation in the NTD inhibited signal transduction from the NTD to the CTD, precluding release of the protein from the DNA, or that a mutation in the NTD caused a conformational change in the CTD of the protein resulting in tighter DNA binding. To analyze the quantitative DNA binding capability of these two variants in the presence and absence of AHL, fluorescence anisotropy was performed.

Materials and Methods:

Protein purification

E. coli Top10 cells (32) harboring a plasmid (pHMGE) encoding EsaR with an N-terminal fusion to a 6X histidine tagged maltose binding protein (MBP) followed by a TEV protease recognition sequence and 5X glycine spacer (HMGE) and variant forms of EsaR similarly tagged (Table 2.1) were grown in Luria-Bertani medium (10 g/L tryptone, 5 g/L yeast extract, 5 g/L NaCl) containing 100 μg/ml ampicillin. Cells were incubated with shaking (200 rpm) at 30^{o}C. IPTG (1 mM) was used to induce protein expression at an OD_{600} of 0.5. Following induction, cells were incubated with shaking (200 rpm) for 4 hours at 25^{o}C. Cultures were centrifuged at 7,000 rpm using a Beckman Coulter JA-10 rotor (Beckman Coulter) for 10 min at 4^{o}C after which the supernatant was decanted. The resulting pellet was resuspended in nickel purification wash buffer (500 mM NaCl, 20 mM HEPES, 20 mM imidazole, 10% glycerol, [pH 7.4]) and passed thrice through a French press at 18,000 psi. The lysate was cleared via ultracentrifugation at 40,000 rpm using a Beckman Coulter 70Ti rotor for 60 min at 4^{o}C. The cleared lysate was filtered with a 0.2 μm pore-size syringe filter (Fisher Scientific) and passed over a Ni-NTA column (GE Healthcare HisTrap HP, 5 ml). Non-specific protein was removed from the column using the nickel purification wash buffer. Histidine-tagged protein was eluted with a 25 ml linear gradient of nickel purification wash buffer containing 20 mM to 500 mM imidazole. Elution fractions were pooled and passed over a heparin

column (GE Healthcare HiTrap HP, 5 ml). Protein was eluted with a 25 ml linear gradient of 10 mM $NaH_2{*}PO_4{*}H_2O$, pH 7.4 containing 400 mM to 800 mM NaCl , as previously described (53). Elution fractions containing HMGE or variant forms of EsaR were pooled, concentrated and passed through a gel filtration column (GE Healthcare HiPrep 26/60 Sephacryl S-200 HR) equilibrated with HMGE working buffer (500 mM NaCl, 20 mM HEPES, 10% glycerol, pH 7.4). Fractions were visualized on a 12% SDS-PAGE gel and those containing a protein with the predicted molecular weight of HMGE (~73 kDa) were pooled, concentrated with an Amicon ultrafiltration unit with a 10,000 molecular weight cut off filter, aliquoted and stored at -70^{o}C.

Construction of the TAMRA-labeled and unlabeled *esa* box

Fluorescence anisotropy assays were developed following established protocols (44, 62). 5' TAMRA NHS ester-labeled DNA (PesaR28 TAMRA) and its unlabeled complement (PesaR28R) were obtained from Integrated DNA Technologies (Table 2.2). Oligonucleotides were resuspended in annealing buffer (100 mM potassium acetate, 30 mM HEPES [pH 7.5]). The concentration of resuspended oligonucleotides was determined by measuring Abs_{260} and using the primer-specific extinction coefficient. Equimolar concentrations of complementary oligonucleotides were annealed by heating to 94^{o}C and slowly cooling to room temperature for the construction of the double-stranded TAMRA-labeled *esa* box (T-esabox). Preliminary fluorescent excitation and emission scans of the T-esabox indicated optimal excitation and emission wavelengths at 580 and 590 nm, respectively. However, due to the considerable overlap of these wavelengths and filter limitations, excitation and emission wavelengths of 540 and 590 nm, respectively, were used for experiments.

An unlabeled dsDNA *esa* box (esabox) was created as described above using oligonucleotides PesaR28 and PesaR28R (Table 2.2).

Fluorescence anisotropy assays

Reagents and materials (buffers, tubes, etc.) used for fluorescence anisotropy assays were kept on ice until fluorescence readings were taken. HMGE or EsaR* variant forms of the protein at concentrations ranging from 0 to 100 nM were incubated with 3 nM T-esabox (concentration of dsDNA). The reaction volume and buffer constituents were kept constant (final conditions of 150 mM NaCl, 6 mM HEPES, 17.5 mM Tris, 3% glycerol, pH 7.6) by using a constant amount of protein and HMGE working buffer as well as a constant amount of 25 mM Tris (pH 7.4) and T-esabox. For a given protein concentration, a 90 μl reaction was created from which 40 μl was aliquoted into two adjacent wells of a Corning 384 well black bottom plate. Plates were placed into a Tecan Infinite F200 Pro fluorometer maintained at 25^{o}C. After 10 min of temperature equilibration, fluorescence anisotropy was measured with an integration time of 100 msec and a G factor of 1. A second reading was taken after 20 min of temperature equilibration under the same conditions. This same set up was performed in triplicate. For each experiment background fluorescence was subtracted from the resulting data to obtain Δ fluorescence anisotropy (Δ FA). For each of the two experiments performed in triplicate, the average Δ FA was calculated. The standard deviation was calculated for the resulting three averages. The reported dissociation constant (Kd) is the average of the three averages. A fit curve and Kd were generated using Equation 1 and XL Fit

Equation 1: anisotropy= $(((AB-AF)/(2*DNA))*(((DNA+x)+Kd)-(((((DNA+x)+Kd)^{2})-((4*DNA)*x))^{0.5})))$

AB is bound T-esabox, AF is unbound T-esabox and DNA is the concentration of T-esabox.

Similar experiments were performed in the presence of 1 μM to 8 μM N-3-oxo-hexanoyl-L-homoserine lactone (Sigma), from which it was determined that 1 μM was sufficient for saturation. This concentration of AHL was used for subsequent experiments.

As a control, unlabeled *esa* box (0-250 nM) prepared as described above was titrated into solution containing 15 nM HMGE and 3 nM T-esabox maintained in 150 mM NaCl, 6 mM HEPES, 17.5 mM Tris, 3% glycerol, pH 7.6 (Table 2.2). A fit was generated and a Ki calculated using Equation 2, as previously described (93).

Equation 2: $\Delta A=(\Delta A_T([I]/Ki)/(1+[I]/Ki+E_T/Kd))$

ΔA is the change in fluorescence anisotropy, ΔA_T is the total change in fluorescence anisotropy, [I] is the concentration of unlabeled DNA, Ki is the inhibition constant, E_T is the concentration of HMGE, Kd is the dissociation constant of HMGE. After obtaining Δ FA, the change in anisotropy as the result of binding of the unlabeled DNA (DNAu) was calculated. This was done by subtracting the anisotropy value obtained at [DNAu]=0 from each data point. The resulting values were used to generate a fit using Equation 2. The same experiment was performed in duplicate.

Results and Discussion:

Using fluorescence anisotropy, the Kd of HMGE and EsaR* variants relative to one another was determined in the presence and absence of AHL. The Kd of HMGE exposed to 1 μM, 2 μM, 4 μM and 8 μM AHL were first compared from which it was observed that they were approximately equal (Figure 2.1). From this it was concluded that of the concentrations of AHL tested, 1 μM AHL was sufficient for saturation and was used for subsequent experiments.

As a control to verify that HMGE was attracted to the *esa* box and not the TAMRA probe, a DNA competition assay was performed. The results demonstrate that anisotropy decreases with increasing concentrations of unlabeled *esa* box, suggesting that the unlabeled *esa* box can compete with T-esabox (Figure 2.2).

The fluorescence anisotropy results after 20 min of room temperature equilibration of the protein samples proved more replicable than those of 10 min room temperature equilibration. Consequently, the reported Kd for each variant is after 20 min of room temperature equilibration (Figure 2.3). The Kd of HMGE in the absence of AHL was determined to be 3.13 +/- 0.33 nM and 6.30 +/- 1.31 nM in the presence of AHL. The Kd of HMGE in the absence of AHL determined by fluorescence anisotropy is in fair agreement with the previously reported Kd of EsaR (53) and is in good agreement with that of other LuxR repressors (10).

The P_{luxI}-gfp assay indicated that A32V is incapable of binding AHL. Consequently, fluorescence anisotropy was performed on A32V as a control to verify that the Kd in the presence and absence of AHL remained constant. The constant Kd for A32V in the presence (2.33 +/- 1.06 nM) versus absence (2.18 +/- 0.73 nM) of AHL further confirms that DNA binding affinity of A32V is not affected by AHL.

Because two variants (D83E, F94Y) were shown to bind AHL but remain unresponsive to it, it was hypothesized that these two variants were incapable of transducing the NTD ligand detection signal to the CTD. The Kd for D83E in the absence of AHL was 4.01 +/- 1.13 nM and 2.91 +/- 0.58 nM in the presence of AHL. Similarly, the calculated Kd for F94Y in the absence of AHL was 3.26 +/- 0.93 nM and 2.65 +/- 1.03 nM in the presence of AHL. Because the Kd of these two variants was similar in the presence and absence of AHL, they appear to have lost the ability to transduce NTD ligand detection to the CTD. The inability of these variants to transduce the signal of AHL detection from the NTD to the CTD, while retaining the ability to bind AHL and DNA suggests that the binding of AHL as well as binding of DNA is an uncoupled process. Homology modeling to TraR and EsaR (M. Churchill, personal communication) suggested that these residues are both surface exposed on a monomer of EsaR. Structural studies on these variants may provide insight as to conformational deviation from the wild type, potentially confirming the mechanism of these results.

It has been speculated, but difficult to biochemically demonstrate, that LuxR homologues transduce a signal from the NTD to the CTD as a result of ligand detection. This interdomain signal causes an alteration in DNA binding as a result of AHL detection, allowing for activators to bind DNA and repressors to dissociate from DNA in the presence of AHL. It has previously been shown that the CTD of LuxR homologues is not required for AHL binding, suggesting that the functionality of the NTD is independent of the presence of the CTD (15). In this study, two mutated residues in EsaR (D83E, F94Y) rendered variant forms of EsaR capable of binding AHL but unresponsive to it. The results of fluorescence anisotropy suggest that these two variants retain the ability to bind DNA in the presence of AHL at levels comparable to the wild type. Because these two variants can bind AHL and retain DNA binding capability comparable to the wild type, it would appear that these two variants are incapable of transducing the signal of AHL binding from the NTD to the CTD. This is one of the first pieces of biochemical evidence that suggests that a LuxR homologue transduces a signal from the NTD to the CTD as a function of AHL detection.

Table 2.1. Strains and plasmids used in this study.

Strain or plasmid	Relevant information	Source or reference
E. coli Top 10	F^- *mcrA* Δ(*mrr-hsdRMS-mcrBC*) ϕ80d*lacZ*ΔM15 Δ*lacX74* *deoR recA1 araD139* Δ(*ara-leu*)*7697* *galU galK rpsL* (Str^r) *endA1 nupG*	(32)
pHMGE	*attb*-His_6-MBP-TEV-Gly_5-*esaR-attb* (HMGE); destination vector in Gateway system	(70)
pHMGEA32V	HMGE with mutation A32 changed to V32	(68)
pHMGED83E	HMGE with mutation D83 changed to E83	(68)
pHMGEF94Y	HMGE with mutation F94 changed to Y94	(68)

Table 2.2. Oligonucleotides used in this study.

Oligonucleotide Name	Oligonucleotide Sequence (5'-3')	Tm (^{o}C)	Source or reference
PesaR28TAMRA	TAMRA-TCTTGCCTGTACTATAGTGCAGGTTAAG	57.8	This study
PesaR28R	CTTAACCTGCACTATAGTACAGGCAAGA	57.8	(53)
PesaR28	TCTTGCCTGTACTATAGTGCAGGTTAAG	64.6	(53)

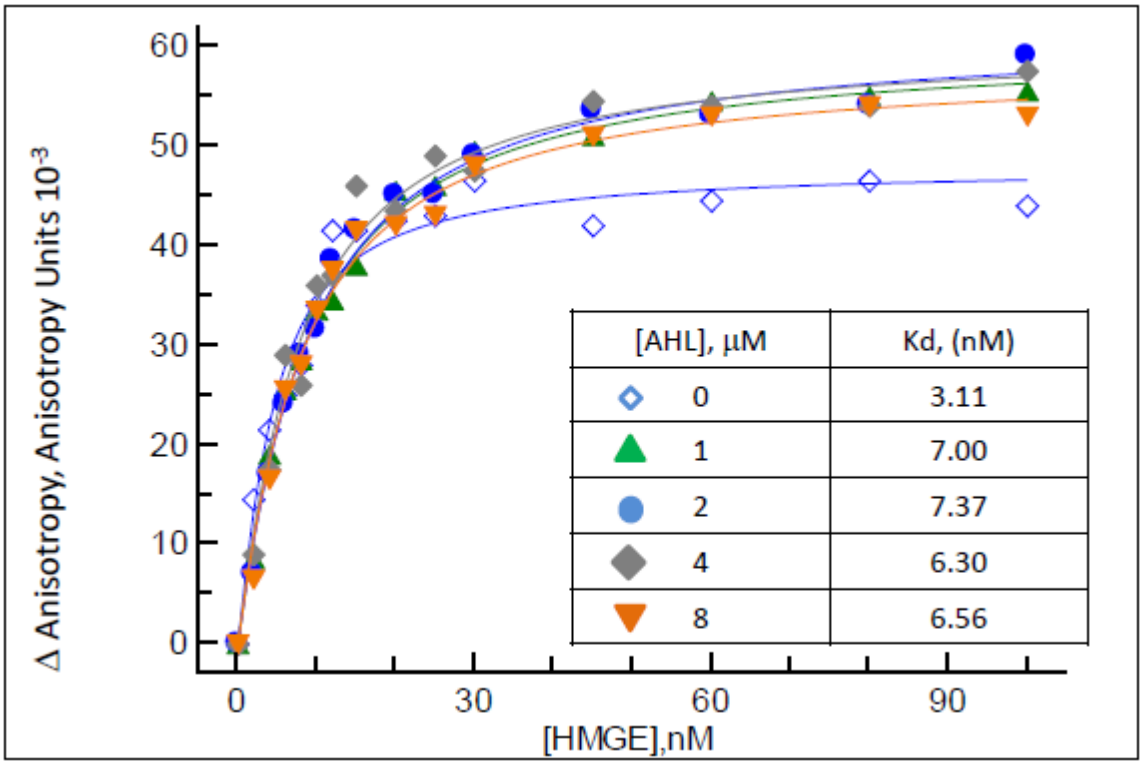

Figure 2.1. In vitro AHL saturation binding assay. Various protein concentrations (0-100 nM) of HMGE were incubated with 3 nM T-esabox (dsDNA concentration) for 20 min at 25°C in the presence of 1, 2, 4, 8 μM AHL. Fluorescence anisotropy was measured with a Tecan F200 Pro fluorometer with a G factor of 1 and excitation and emission wavelengths of 540 and 590 nm, respectively. Background anisotropy was subtracted and the resulting data were used to generate a fit curve and calculate the apparent Kd.

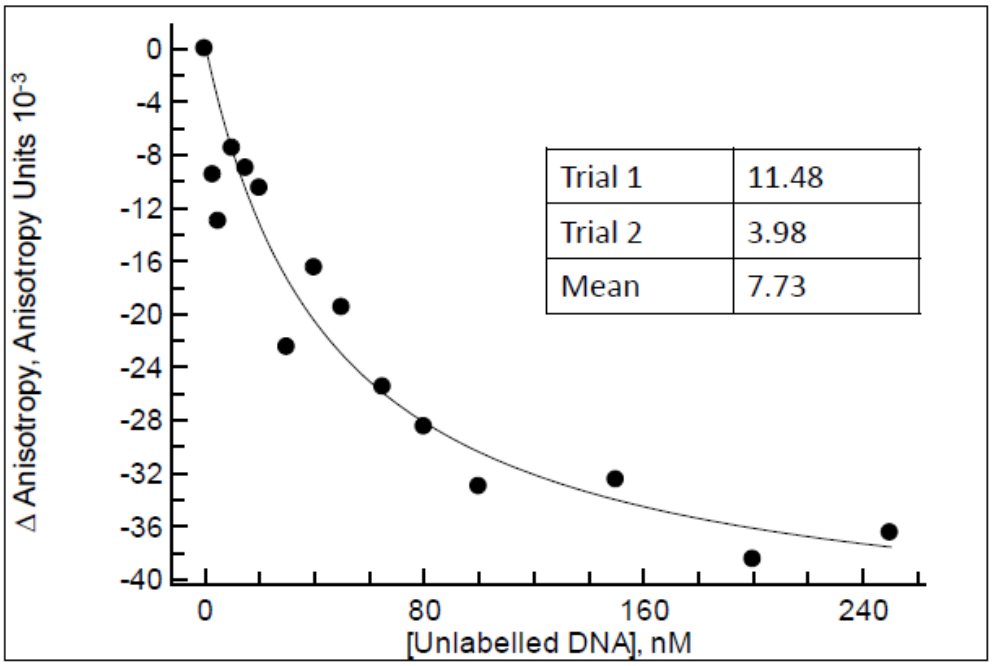

Figure 2.2. Unlabeled *esa* box competition control. 0-250 nM unlabeled esabox was titrated into reactions containing 15 nM HMGE and 3 nM T-esabox. After incubation at 25°C for twenty min, fluorescence anisotropy was measured with a Tecan Infinite F200 Pro fluorometer with a G factor of 1 and excitation and emission wavelengths of 540 and 590 nm, respectively. Plot shown is the average of experiments performed in duplicate with the Ki obtained from individual experiments. The table indicates the Ki (nM) obtained from each of the two trials and the mean of both trials.

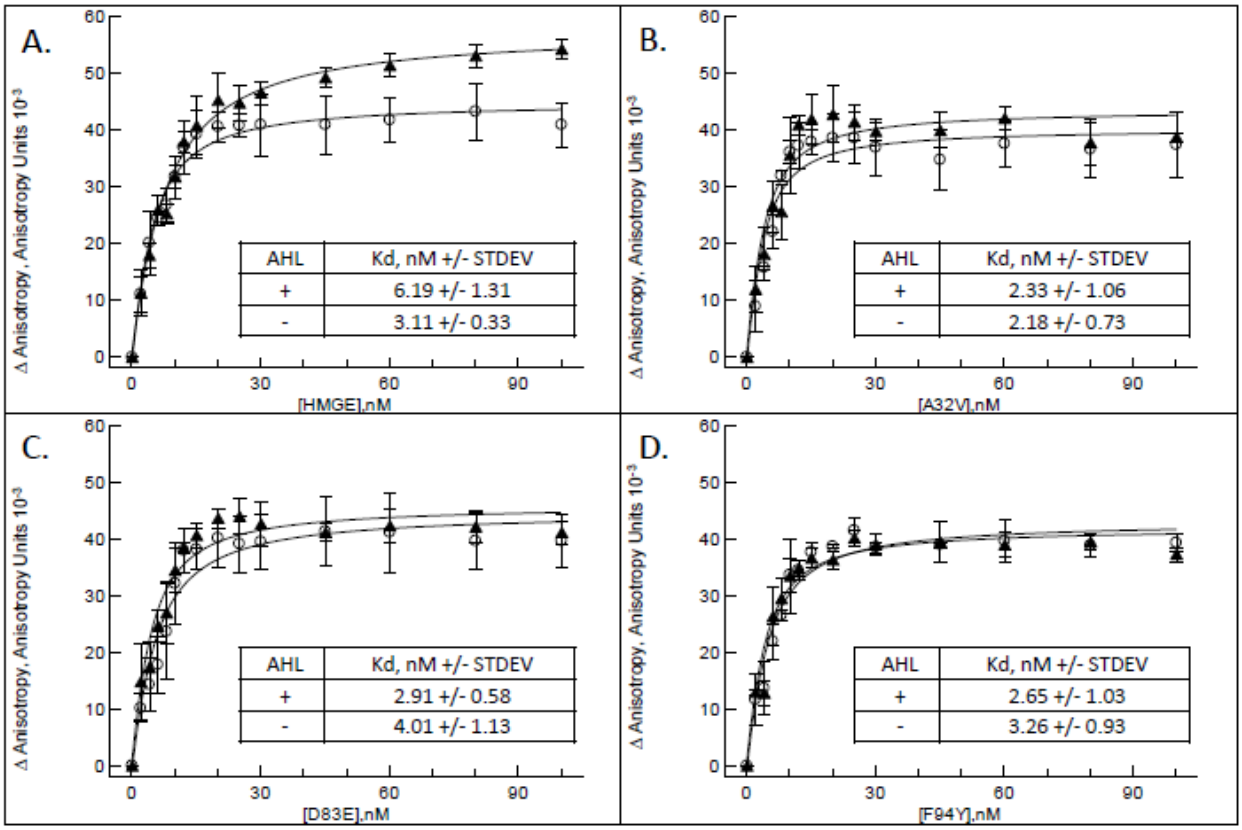

Figure 2.3. *In vitro* relative binding affinities of HMGE and EsaR* variants. Various protein concentrations (0-100 nM) of HMGE (A), A32V (B), D83E (C), F94Y (D) were incubated with 3 nM T-esabox (dsDNA concentration) for 20 min at 25°C in the presence (triangles) and absence (circles) of 1 μM AHL. Fluorescence anisotropy was measured with a Tecan F200 Pro fluorometer with a G factor of 1 and excitation and emission wavelengths of 540 and 590 nm, respectively. Background anisotropy was subtracted and the resulting data were used to generate a fit curve and calculate the apparent Kd. Duplicate samples analyzed from experiments performed in triplicate. Average of and standard deviation across three experiments for each protein is shown.

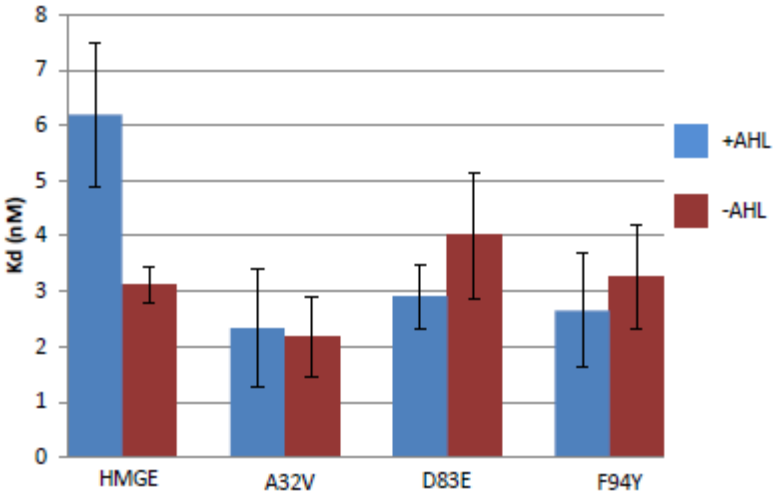

Figure 2.4. Relative Kd values for HMGE and EsaR* variants. Fluorescence anisotropy (Figure 2.3) was performed on HMGE and EsaR* variants. Duplicate samples were analyzed from experiments performed in triplicate. Average of and standard deviation across three experiments for each protein is shown.

Chapter III

Biochemical Analysis of the EsaR N-terminal Domain

Portions of this chapter were published in (70)

Abstract:

The majority of LuxR homologues function only in the presence of their cognate acyl-homoserine lactone (AHL). EsaR represents a subset of LuxR homologues that are active in the absence of AHL and are inactivated by its presence. The LuxR homologue TraR has been shown to require AHL for dimerization as well as protease resistance. To assess if AHL has the same impact on EsaR, protease susceptibility and quaternary structure were investigated in the absence and presence of AHL. Pulse-chase experiments demonstrated that AHL, added co-translationally or post-translationally, does not impact the protease susceptibility of EsaR. Limited proteolytic digestions also suggested that inter and intra-domain conformational changes occur within EsaR as a result of ligand binding. Gel filtration and crosslinking experiments demonstrated that EsaR remains dimeric in both the absence and presence of AHL and that the N-terminal domain of EsaR alone is sufficient for dimerization. It is the crosslinking experiments utilizing the EsaR N-terminal domain that are the specific focus of this chapter.

Introduction:

Despite the widespread presence of LuxR homologues amongst proteobacteria, the basic question of how acyl-homoserine lactone (AHL) detection transduces a signal that alters the activity of the transcription factor remains unresolved. Due to protein solubility issues, structural information for LuxR homologues is limited. A few structures are available, but several are of only the ligand-binding domain and all are only in the presence of their cognate AHL or an antagonist (6, 12, 45, 82, 94, 96). In some cases, removal of the CTD has allowed for improved solubility necessary for structural analysis; it would appear that the CTD is an antagonist of solubility (6, 69, 94). Consequently, it was hypothesized that an EsaR construct lacking the CTD could provide for improved solubility compared to the full-length protein. This construct could then be used to gain structural information about the protein, potentially

delineating conformational changes occurring as a result of ligand binding. One study has described the structure of CviR from *Chromobacterium violaceum* in the presence of its cognate AHL as well as an antagonist. However, the analysis of EsaR described in this study would be the first example of a LuxR homologue for which structural information is provided for both the presence and absence of its native AHL.

Sequence alignments of EsaR clade members to other LuxR homologues have indicated that the EsaR clade has an extended linker region between the NTD and CTD as well as additional residues on the C-terminus (74, 79). For EsaR, this extended linker is comprised of residues 171-178. Because it is unknown whether or not the extended linker holds significance in regards to dimerization as well as flexibility, two EsaR constructs were developed and biochemically examined. The first construct, NTD169, includes residues 1-169 and lacks the extended linker region. The second construct, NTD178, includes residues 1-178 and includes the extended linker region (Figure 3.1). These constructs were analyzed for their ability to bind AHL and for their ability to dimerize.

Materials and Methods:

NTD169 and NTD178 construct development

Using pHMGE (70) as the DNA template, the forward primer ATTBTEV (Integrated DNA Technologies) (Table 3.1) and the reverse primer ATTBR169 or ATTBR178 (Integrated DNA Technologies) (Table 3.1) were used to amplify PCR products that contained *attB*-TEV recognition sequence-Gly_5-*esaR* (residues 1-169 or 1-178)-*attB* (Table 3.1). The resulting product was incubated with dATP and *Taq* polymerase at 72^{o}C for 20 min. A Qiagen PCR purification kit was used to remove unbound dATP and *Taq* polymerase. The PCR product was then ligated into pGEM-T easy (Promega) and was transformed into *E. coli* DH5α cells (34). Purified plasmid DNA was submitted to the Virginia Bioinformatics Institute (VBI) (Blacksburg,

VA) for sequencing. After confirming sequence integrity, the plasmid was subjected to the BP reaction of Gateway cloning into the donor vector pDONR201, conferring kanamycin resistance (Kn^r), following the vendor's protocol (Invitrogen). DH5α cells were transformed with the resulting plasmid and plated onto agar plates containing 50 μg/ml kanamycin. A viable colony was grown overnight in 5 ml LB supplemented with 50 μg/ml Kn. Plasmid DNA was extracted from these cells using a Qiagen miniprep kit. Purified DNA was then subjected to the LR reaction of Gateway cloning (Invitrogen) into the destination vector pDEST-HisMBP (55) to create pHMGNTD169 and pHMGNTD178, respectively. These plasmids were transformed into *E. coli* BL21 DE3 (Stratagene) and purified plasmid DNA was sequenced to confirm integrity (VBI).

NTD169 and NTD178 protein purification

E. coli BL21 DE3 cells (Stratagene) harboring pHMGNTD169 or pHMGNTD178 were grown in Luria-Bertani medium (10 g/l tryptone, 5 g/l yeast extract, 5 g/l NaCl) containing 100 μg/ml ampicillin (Ap). Cells were incubated with shaking (200 rpm) at 30^{o}C. IPTG (1 mM) was used to induce protein expression at an OD_{600} of 0.5. Following induction cells were incubated with shaking (200 rpm) overnight at 19^{o}C. Cultures were centrifuged at 7,000 rpm using a Beckman Coulter JA-10 rotor (Beckman Coulter) for 10 min at 4^{o}C after which the supernatant was decanted. The resulting pellet was resuspended in nickel purification wash buffer (500 mM NaCl, 20 mM HEPES, 20 mM imidazole, 10% glycerol [pH 7.4]) and passed thrice through a French press at 18,000 lb/in^2. The lysate was cleared by ultracentrifugation at 40,000 rpm in a Beckman 70Ti ultra rotor at 4^{o}C for 1 hr. The cleared lysate was filtered with a 0.2 μm-pore size syringe filter (Fisher Scientific) and passed over a 5 ml HisTrap HP Ni-NTA column (GE Healthcare). Non-specific protein was removed from the column using the nickel purification wash buffer. Histidine-tagged protein was eluted using a 25 ml linear gradient of nickel purification wash buffer and nickel purification elution buffer (500 mM NaCl, 20 mM HEPES, 500 mM imidazole, 10%

glycerol, pH 7.4). Elution fractions were pooled and passed over amylose resin following the vendor's protocol (New England Biolabs). Eluted protein was subsequently passed over a HiPrep 26/60 Sephacryl S-200 HR column (GE Healthcare) equilibrated with HMGE working buffer (500 mM NaCl, 20 mM HEPES, 10% glycerol [pH 7.4]). Fractions were visualized on a 12% SDS-PAGE gel. Fractions containing HMGNTD169 or 178 were pooled and dialyzed against an excess of nickel purification wash buffer in the presence of TEV protease at 4^{o}C overnight. The sample was then passed over the 5 ml HisTrap HP Ni-NTA column. The flowthrough (containing cleaved NTD169 or 178) was collected and passed over amylose resin following the vendor's protocol (New England Biolabs). The flowthrough was then passed over the Sephacryl S-200 column equilibrated with HMGE working buffer. Eluted protein was visualized on a 12% SDS-PAGE gel and fractions containing protein with the predicted molecular weight of a monomer (~20 kDa for NTD169 and ~21 kDa for NTD178) were pooled, concentrated, aliquoted and stored at -70^{o}C until needed. Total mass analysis was performed on NTD178 (Virginia Tech-Mass Spectrometry Incubator).

Partial digestion: *in vitro* proteolysis by thermolysin

EsaR NTD169 or NTD178 (13.5 μM) was exposed to decreasing concentrations of thermolysin. At each concentration of thermolysin, digestions were performed in the absence or presence of AHL (67.5 μM), in a final concentration of 1X thermolysin buffer (2 mM $CaCl_2$, 5% glycerol, 150 mM NaCl, 10 mM Tris-HCl, pH 8.0). After one hour of incubation at 37^{o}C, reactions were quenched by boiling with1X sample buffer (5X stock contains 0.624 ml 1 M Tris (pH 6.8), 0.2 g SDS, 1.04 ml glycerol, 0.5 ml β-mercaptoethanol, trace bromophenol blue) prior to analysis on a 12% SDS-PAGE gel.

A similar control assay in the presence of thermolysin was performed with BSA (New England Biolabs), in the presence or absence of AHL. BSA (13.5 μM) was exposed to decreasing concentrations of

thermolysin (7.2 μM, 1.69 μM, 0.42 μM). At each concentration of thermolysin, digestions were performed in the absence or presence of AHL (67.5 μM), in a final concentration of 1X thermolysin buffer and a final volume of 25 μl. After one hour of incubation at 37^{o}C, reactions were quenched by boiling with1X sample buffer prior to analysis on a 12% SDS-PAGE gel.

Matrix-assisted laser desorption ionization-tandem time of flight (MALDI-TOF/TOF) mass spectrometry analysis was performed by the Virginia Tech-Mass Spectrometry Incubator on protein fragments of interest.

BS^3 crosslinking

EsaR NTD178 (17.5 μM) was exposed to increasing concentrations (150 to 1250 μM) of a BS^3 crosslinker (Thermo Scientific, Rockford, Illinois). The reaction volume was kept constant with HMGE working buffer for a final volume of 20 μl. Reactions were incubated for 30 min at room temperature. Reactions were stopped using 1 μl 1 M Tris (pH 7.5) and visualized on a 12% SDS-PAGE gel after boiling with sample loading buffer.

EsaRNTD169 or NTD178 (10 μM) was crosslinked with 100 μM BS^3 (Thermo Fisher Scientific) in the absence or presence of 50 μM AHL. The 15 μl reactions were carried out in 20 mM HEPES, 500 mM NaCl, 10% glycerol (pH 7.4) at room temperature and quenched at time points up to 30 min by boiling with sample buffer. The protein was then visualized by 12% SDS-PAGE.

Protein crystallization

Purified NTD169 or NTD178 was concentrated using an Amicon ultrafiltration unit equipped with a 10,000 MWCO filter. Concentrated protein was subjected to a series of chemical conditions (JCSG I and II suite, Wizard I and II conditions) in the presence and absence of 5X AHL (relative to protein concentration) (Table 3.2). Plates were incubated at 8^{o}C and were routinely checked for crystal growth.

Results and Discussion:

Native EsaR has previously been purified (53) but the method is time consuming and has not proven to be easily reproducible (S.B. von Bodman, Personal Communication). Current efforts are focused on the recombinant protein, HMGE, to circumvent solubility issues. This construct contains a 6x Histidine tag, MBP, TEV protease recognition sequence and a 5x Glycine spacer fused to EsaR (Figure 3.1) (70).

Given that the CTD is a common antagonist of solubility in the LuxR family of proteins (6, 94), constructs containing only the EsaR NTD were developed. Truncations of HMGE were generated, extending from residues 1 to 169 or 1 to 178. MBP fusion constructs yielded soluble protein which was readily purified and cleaved by TEV protease (Figure 3.2). Because the NTD constructs could be cleaved nearly to completion with TEV protease whereas HMGE had incomplete cleavage leading to the formation of heterodimers (composed of cleaved and uncleaved protein [D. Schu, Personal Communication]), it appears as though the NTD constructs alleviate TEV cleavage issues previously encountered with HMGE. The NTD was soluble up to 817 μM, whereas native EsaR has been reported to remain soluble only up to 400 μM (53).

A thermolysin partial digest has previously been performed on HMGE in the presence and absence of AHL resulting in differential banding patterns (70). These data suggest that HMGE undergoes a

conformational change in the presence versus absence of AHL, and that HMGE is capable of binding AHL. To verify that the NTD constructs retained AHL binding capability, a similar limited proteolytic digestion assay was employed. Thermolysin is an endopeptidase that recognizes hydrophobic residues. The TraR crystal structure has demonstrated that the AHL binding pocket of that protein is hydrophobic and similar results are seen in other LuxR homologues (6, 94, 96, 97). Because TraR is also a LuxR homologue, it would appear reasonable that the binding pocket of EsaR is also hydrophobic. The results from the thermolysin partial digest on the NTD constructs would suggest that NTD169 and NTD178 are capable of binding AHL as they are more resistant to proteolysis in the presence versus the absence of AHL (Figure 3.3). Thermolysin cleavage of NTD178 incubated with AHL produced two fragments that were not present following thermolysin cleavage of NTD178 in the absence of AHL. MALDI-TOF/TOF analysis of the two EsaR NTD bands of highest molecular weight determined that they were minimally comprised of amino acids 1-160 and 1-93. These regions encompass most of the NTD and the region around the AHL binding site; they appear to be protected from complete thermolysin digestion when AHL is present. Therefore the EsaR NTD appears to be capable of binding AHL, independent of the CTD (Figure 3.3). A similar control experiment was performed using BSA, which has no known ability to bind AHL. The bands resulting from proteolysis were identical for the presence and absence of AHL, confirming that AHL does not alter thermolysin activity (Figure 3.4).

Some LuxR homologues require both the NTD and CTD for stability whereas others require only the NTD (6, 69). To assess if EsaR is stable and capable of forming multimers with only the NTD, crosslinking was performed in the presence and absence of AHL. The preliminary crosslinker concentration optimization experiment demonstrated that a 10X concentration of crosslinker relative to protein concentration provided more distinct bands than a higher concentration of crosslinker (Figure 3.5). Subsequent crosslinking experiments used a 10X concentration of crosslinker relative to protein concentration.

NTD169 displayed only a monomeric band whereas NTD178 displayed both a monomeric and dimeric band in both the presence and absence of AHL, similar to results reported for CarR (90). These crosslinking results suggest that the NTD with the extended linker is capable of dimerization (Figure 3.6). However, the BS^3 crosslinker used functions primarily on lysine residues. There is one lysine residue present in NTD178 that is not present in NTD169, which may explain the differences in the crosslinking results observed between NTD169 and NTD178. Additionally, heterodimers of NTD169 and HMGNTD169 as well as NTD178 and HMGNTD178 have been observed in the elution of amylose resin after TEV cleavage, suggesting that NTD169 is capable of dimerization (data not shown). Thus the differences observed in the crosslinking results of NTD169 and NTD178 may be an experimental artifact.

Development of the EsaR NTD constructs has answered several questions. Both the NTD169 and NTD178 constructs could be almost completely cleaved from MBP using TEV protease, something that has been unsuccessful with HMGE. It could be speculated that the CTD conceals the TEV protease recognition sequence in HMGE. It is also possible that in the HMGE construct, insolubility associated with EsaR cleaved away from MBP drives the formation of heterodimers containing EsaR and HMGE. After TEV cleavage, both NTD169 and NTD178 remain soluble at high concentrations (up to 259 μM NTD169, 817 μM NTD178). Because this has not been replicable with native EsaR (previously reported one time as soluble up to 400 μM in (53) but has not been reproduced), the CTD is likely an antagonist of solubility which supports the hypothesis regarding heterodimer formation of HMGE and EsaR. Crosslinking has demonstrated that NTD169 remains monomeric in the presence and absence of AHL whereas NTD178 forms monomers and dimers in the presence and absence of AHL. However, the observation of heterodimer formation through amylose resin elution suggests that NTD169 or NTD178 are each sufficient for dimerization. The conserved dimeric state of NTD178 in the presence and absence

of AHL observed in crosslinking suggests that AHL does not alter the quaternary structure of EsaR, supporting gel filtration analysis of HMGE +/- AHL (70).

X-ray crystallography is currently being pursued as an option to address what sort of conformational change occurs in the EsaR NTD as a result of AHL-binding. NTD169 and NTD178 have been screened against a series of conditions (Table 3.2) in the presence and absence of AHL. Needle-like crystals have formed under ten different conditions for NTD169 (165 μM) in the absence of ligand (Figure 3.7, Table 3.2). One condition rendered small, hair-like crystals in the presence of AHL for NTD169 (259 μM) (data not shown). This same condition in the absence of AHL caused protein precipitation, suggesting that these crystals may contain the ligand despite its short half-life. Six conditions have produced needle-like crystals for NTD178 (111 μM) in the absence of ligand (data not shown). Additionally, one condition produced cuboid crystals in the absence of ligand (Figure 3.7, Table 3.2). One crystal from this condition was isolated for X-ray diffraction. The results did not produce data from which a structure could be deduced, however, it is known that the cuboid crystal produced is a protein crystal. It is possible that the poor diffraction results were due to the age of the crystals. These crystallization conditions are currently being optimized. No crystals have formed for NTD178 in the presence of AHL.

In summary, early crystallization conditions for the EsaR NTD in the presence and absence of AHL have been established. One sample has been subjected to diffraction analysis. Though the resulting data could not be used to deduce the crystal structure, it was established that the crystal was a protein crystal. Continuing efforts of optimizing crystallization conditions for the EsaR NTD in the absence and presence of AHL should provide improved crystals from which a crystal structure could be solved. These structures would be the first available for a LuxR homologue in both the presence and absence of a cognate AHL. This information could potentially answer the question of what conformational changes

occur as a result of ligand binding that allow the EsaR subset of transcription factors to function in a manner opposite to that of the larger LuxR family.

Table 3.1. List of primers used in this study.

Primer Name	Primer Sequence (5'-3')	Tm (^{o}C)
ATTBTEV	GGGGACAACTTTGTACAAAAAAGTTGTGGAGAACCTGTACTTCCAG	65.6
ATTBR169	GGGGACAACTTTGTACAAGAAAGTTGCATTATCAGGCTCGCTCGCCTTC	74.8
ATTBR178	GGGGACAACTTTGTACAAGAAAGTTGCATTATCATTTGTCCGCGCTCTG	73.1

Table 3.2. NTD169 and NTD178 crystallization conditions.

Protein	Concentration (μM)	+/- AHL[a]	Salt/Buffer	pH	Precipitant/ Other	Well	Ratio (Protein:Solvent)	Description
NTD169	165	-	0.1 M tri-Na citrate	5.5	20% PEG 3000	JCSG A2	1:1	Needle
NTD169	165	-	0.1 M citric acid	5	20% PEG 6000	JCSG B9	1:1	Needle
NTD169	165	-	0.1 M HEPES	7.5	10% PEG 8000	JCSG B4	1:3	Needle
NTD169	165	-	0.1 M BICINE	9	20% PEG 6000	JCSG B3	1:3	Needle
NTD169	165	-	1.1 M Na malonate, 0.1 M HEPES	7	0.5% Jeffamine ED-2001	JCSG F10	1:3	Needle
NTD169	165	-	0.1 M BICINE	9	10% MPD	JCSG F6	3:1, 1:1, 1:3	Needle
NTD169	165	-	0.1 M HEPES	7	30% Jeffamine ED-2001	JCSG G1	1:1, 1:3	Needle
NTD169	165	-	0.2 M Na malonate	7	20% PEG 3350	JCSG G6	3:1, 1:1, 1:3	Needle
NTD169	165	-	0.1 M Ammonium acetate, 0.1 M bis-Tris	5.5	17% PEG 10,000	JCSG H6	1:3	Needle
NTD169	259	-	0.2 M Zn acetate, 0.1 M Na cacodlyate	6.5	10% isopropanol	JCSG E7	1:1	Needle
NTD169	259	+	0.15 M DL-Malic acid	7	20% PEG 3350	JCSG G8	1:1	Small needle
NTD178	111	-	0.1 M tri-Na citrate	5.5	20% PEG 3000	JCSG A2	1:3	Needle
NTD178	111	-	0.2 M di-Ammonium citrate	5	20% PEG 3350	JCSG A3	1:3	Needle
NTD178	111	-	0.2 M Na thiocyanate	6.9	20% PEG 3350	JCSG B2	1:3	Needle
NTD178	111	-	0.14 M $CaCl_2$, 0.07 M Na acetate	4.6	14% isopropanol, 30% glycerol	JCSG D11	1:1	Cuboid
NTD178	111	-	0.2 M KCl, 0.05 M HEPES	7.5	35% Pentaerythritol propoxylate (5/4 PO/OH)	Wizard E8	1:3	Needle
NTD178	111	-	0.2 M Ammonium sulfate, 0.1 M HEPES	7.5	25% PEG 3350	Wizard F8	1:3	Needle
NTD178	111	-	0.2 M Lithium sulfate monohydrate, 0.1 M bis-Tris	6.5	25% PEG 3350	Wizard G3	1:1, 1:3	Needle

[a]Concentration relative to protein concentration.

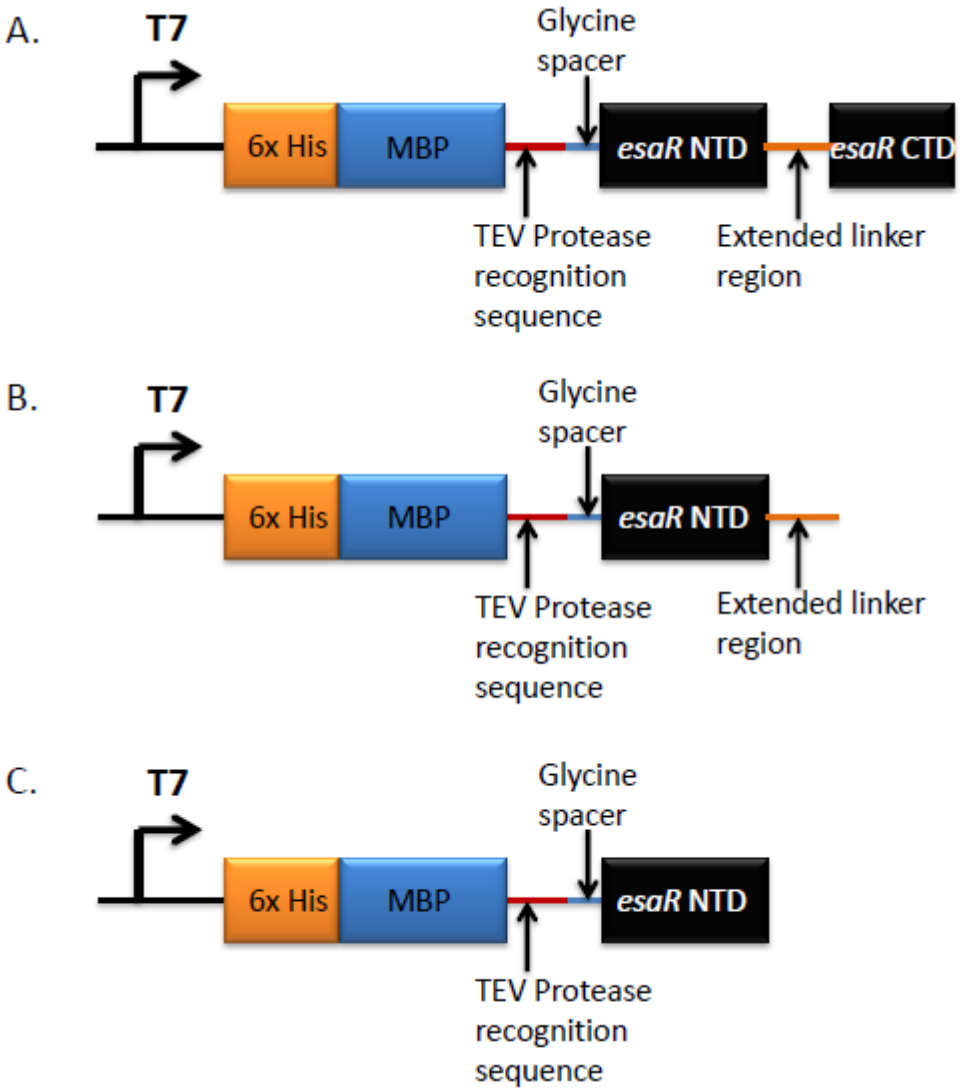

Figure 3.1. Cartoon depiction of HMGE and EsaR NTD constructs. HMGE (A), NTD178 (B), NTD169 (C).

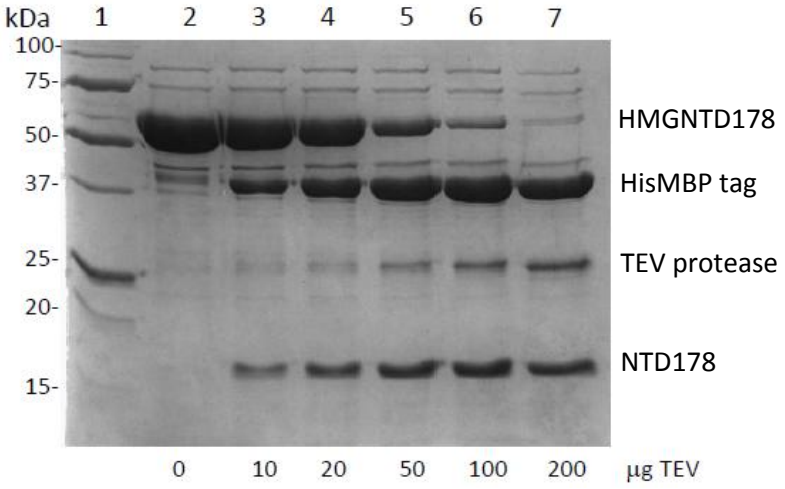

Figure 3.2. NTD178 TEV protease digestion assay. Purified NTD178 fused to MBP (~0.62 mg) was incubated with TEV protease for 24 hours at 4^{o}C while dialyzing against HMGE working buffer. Samples were: 1, size standards; 2-7, ~0.62 mg NTD178 incubated with indicated amount of TEV protease indicated below gel.

A.

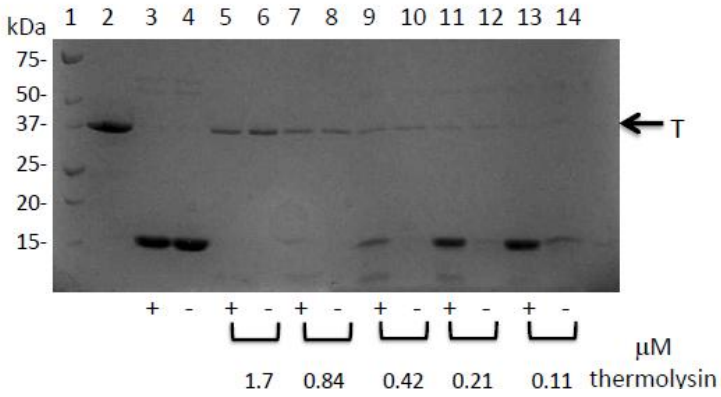

B.

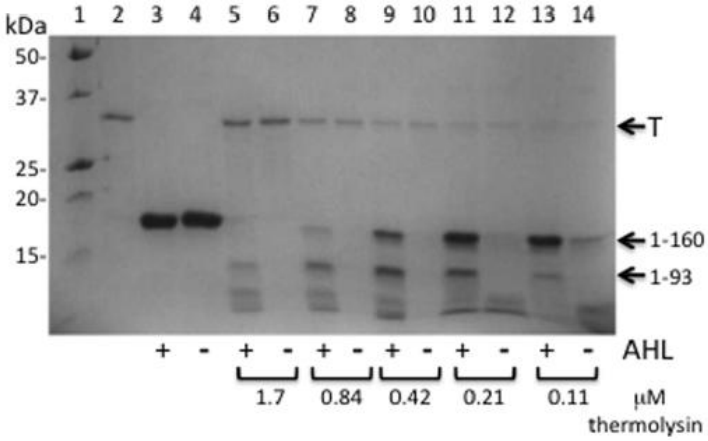

Figure 3.3. Ability of EsaR NTD169 and NTD178 to resist thermolysin digestion. Purified NTD169 (A) or NTD178 (B) was used at a final concentration of 13.5 µM. Samples were; 1, size standards; 2, thermolysin (T); 3-4, NTD +/- AHL; 5-14, NTD +/- AHL and digested with the indicated concentration of thermolysin. The images are representative of experiments performed in duplicate.

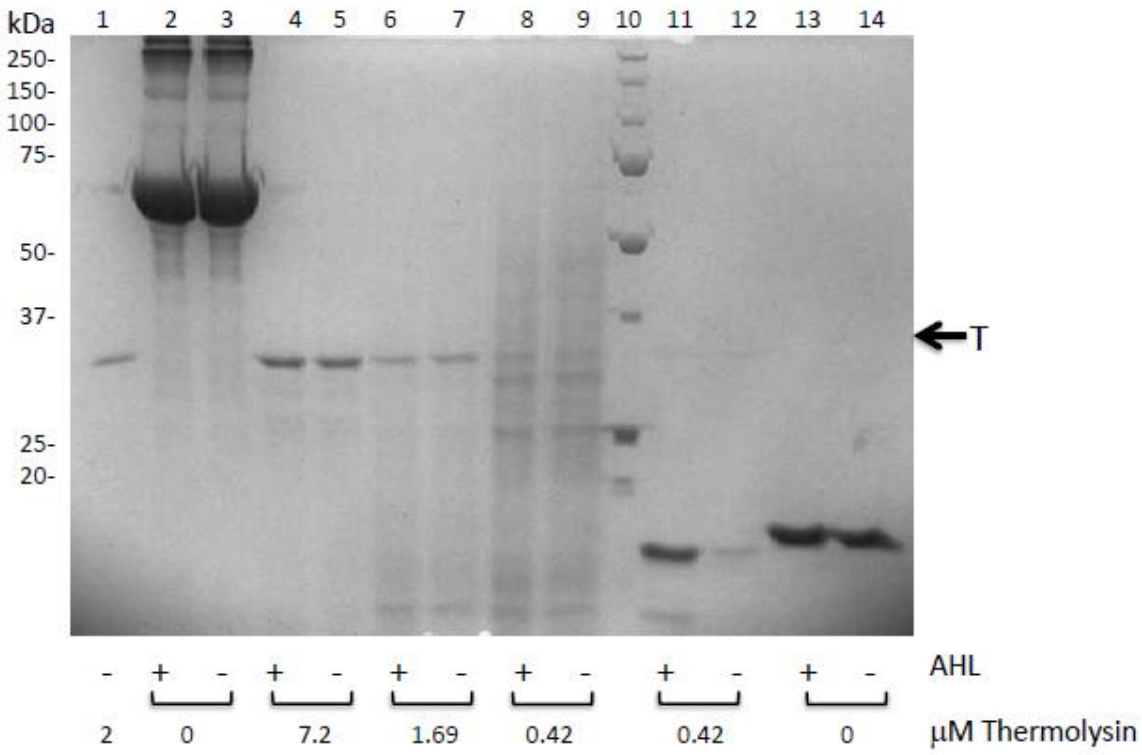

Figure 3.4. Ability of BSA to resist thermolysin digestion. BSA or NTD178 was used at a final concentration of 13.5 μM. Samples were; 1, thermolysin (2 μM, T); 2, BSA + AHL; 3, BSA – AHL; 4-9 BSA +/- AHL and digested with the indicated concentration of thermolysin; 10, size standards; 11-14, NTD178 +/- AHL and digested with the indicated concentration of thermolysin. The image is representative of experiments performed in duplicate.

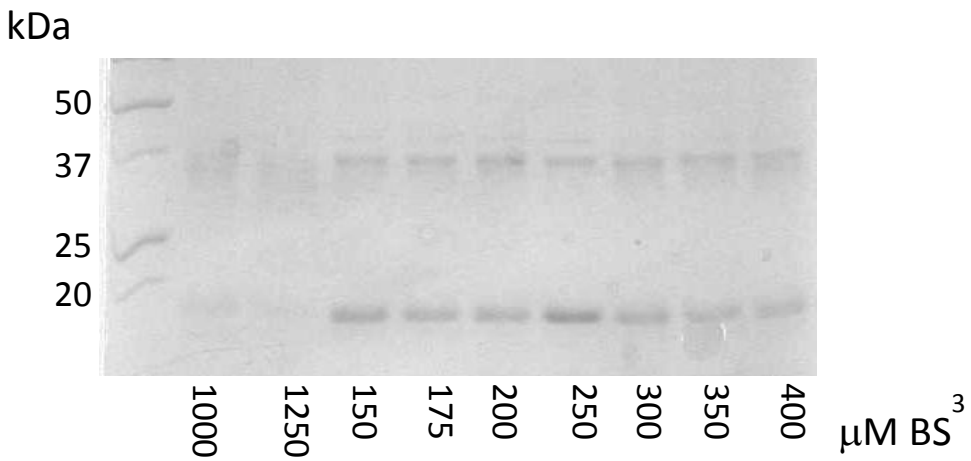

Figure 3.5. Preliminary BS^3 crosslinker concentration optimization. NTD178 (17.5 μM) was exposed to varying concentrations of BS^3 crosslinker as indicated. Reactions were incubated at room temperature for 30 min and were quenched by boiling with sample buffer.

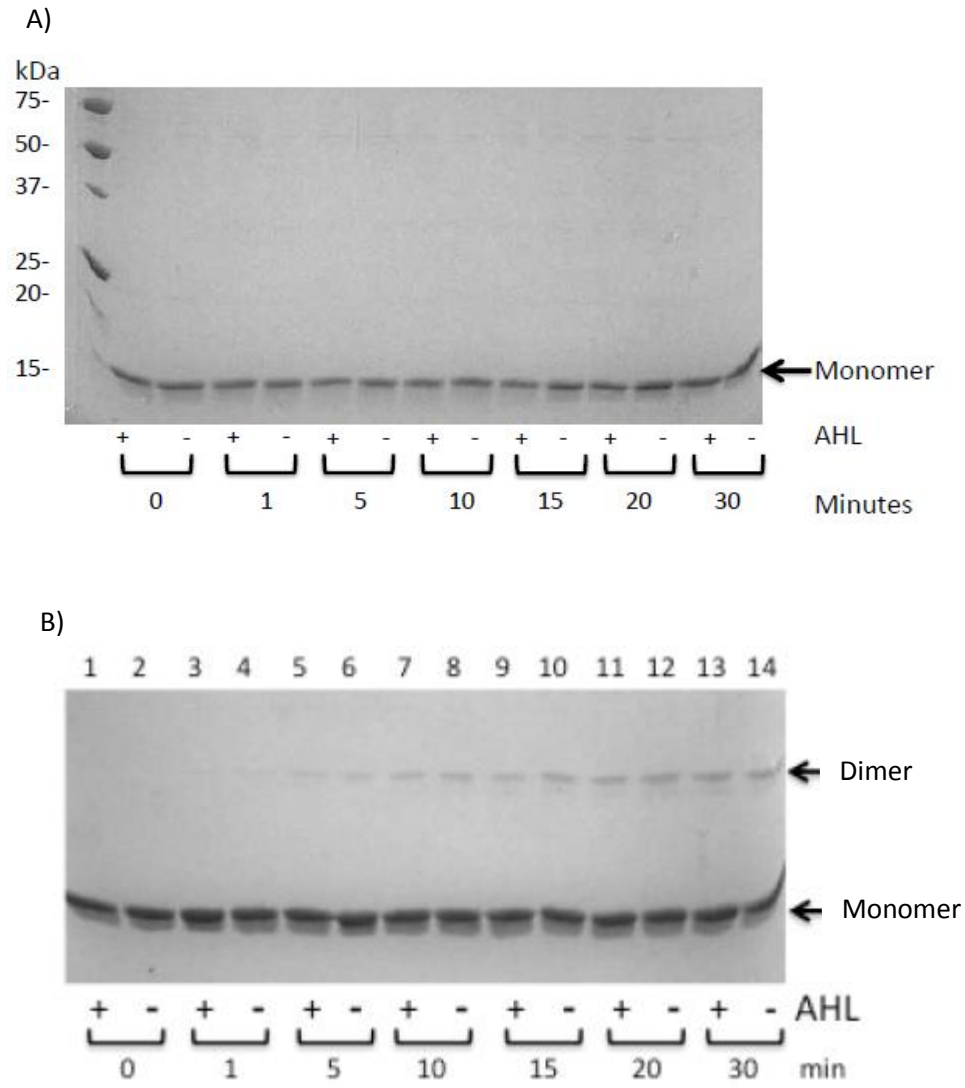

Figure 3.6. Ability of EsaR NTD169 and NTD178 to form dimers. of NTD169 (A) or NTD178 (B) at a 10 μM concentration were exposed to 100 μM BS^3 crosslinker in the presence (+) and absence (-) of AHL. Reaction pairs, left to right, correlate to 0, 1, 5, 10, 15, 20, 30 min. The images are representative of experiments performed in duplicate.

A) 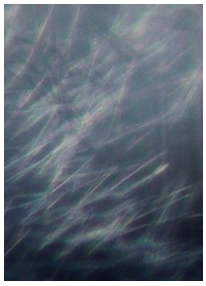

B) 

Figure 3.7. EsaR NTD representative crystals. “Needle-like” crystals (A) were grown for NTD169 in the absence of AHL. “Cuboid” crystals (B) were grown for NTD178 in the absence of AHL.

Chapter IV

Overall Conclusions

Biochemical analysis of LuxR homologues has traditionally proven difficult in large part due to protein solubility issues. In an attempt to develop a soluble EsaR construct lacking a fusion tag, the EsaR NTD was investigated. Two EsaR NTD constructs were created; one contained the extended linker region unique to the EsaR subset of LuxR homologues, the other construct lacked the extended linker region. Both constructs were expressed as C-terminal fusions to MBP containing a histidine tag to facilitate purification efforts and enhance solubility. After the fusion protein was purified, it was incubated with TEV protease to remove His-MBP. Cleavage efficiency was nearly 100%, something that has not been observed with the full-length version of EsaR fused to MBP. The cleaved NTD proved to be soluble to high concentrations, also something that has not proven easily replicable for full-length EsaR.

Crosslinking and thermolysin partial digestions assays were performed to verify that the purified EsaR NTD constructs retain biological activity, namely multimerization and AHL retention. Thermolysin partial digests confirmed that both constructs, NTD169 and NTD178 were capable of binding AHL, establishing that the extended linker region is not required for AHL retention. Crosslinking assays demonstrated that NTD178 is capable of dimerization, suggesting that the CTD is not required for dimerization. Additionally, the crosslinking assays demonstrated that the dimeric state of NTD178 is conserved in the absence or presence of AHL. NTD169 was not capable of dimerization based on the crosslinking assays. However, unreported results have shown that NTD169 is capable of forming heterodimers with NTD169 fused to MBP, suggesting that the lack of dimerization observed in crosslinking assays is an experimental artifact.

Because both NTD169 and NTD178 remained soluble at high concentrations, these proteins were subjected to structural studies. A 1D NMR spectrum for NTD178 was obtained, from which no structural features could be deduced. Preliminary protein crystallization screens produced protein crystals for NTD169, shifting the focus of structural studies from NMR to X-ray crystallography. Protein crystals

have been formed for NTD169 and NTD178 in the absence and presence of AHL. One condition for NTD178 in the absence of AHL produced relatively robust crystals which were subjected to diffraction analysis. A structure could not be deduced from the resulting data, but it did confirm that the crystal was composed of protein. Future studies could optimize the early crystallization conditions produced to obtain better crystals from which a crystal structure could be solved.

Studies involving variant forms of EsaR that are unresponsive to AHL have demonstrated that two residues have a critical role in binding AHL, but remain unresponsive to it (D83E, F94Y). Because the Kd of these two variants was not different in the presence and absence of AHL, but retain AHL-binding capability, it is possible that they are incapable of transducing a signal from the NTD to the CTD in response to AHL binding. Once the EsaR NTD crystal structure is solved, performing X-ray crystallography on these variants in the presence and absence of AHL may give some indication of how this mechanism works.

Of the several LuxR homologue structures solved, a common point of contention is the dimerization interface. The dimerization interface of TraR from *Agrobacterium tumefacians* is asymmetrical (82, 96), unlike the symmetrical dimerization interface of LasR from *Pseudomonas aeruginosa* (6). A unique inter-domain dimerization interface has recently been solved for the QscR structure of *Pseudomonas aeruginosa* in which dimerization contacts are made between the NTD and CTD. Given the lack of conservation in the dimerization interface, EsaR residues could be identified based on the aforementioned structures and mutated in an attempt to gain information regarding the EsaR dimerization interface.

Discoveries of protein-protein interactions in Q-S systems are increasing, both as anti-activators and anti-repressors (28, 47, 71). Such interactions are difficult to predict based on sequence alignments due

to the low sequence identity amongst anti-regulators. Given this, investigation of an EsaR anti-regulator could also be a possible future project.

The detection of AHL by a cognate transcription factor is one of the most fundamental principles of QS. It is only with a proper understanding of the AHL-transcription factor relationship that QS-dependent processes could be exploited, holding practical applications especially for therapeutic applications. One of the primary focuses of this research was to investigate the AHL-EsaR relationship. The results from this research have helped to answer some interesting questions, giving a better understanding of this relationship. These results may not only hold relevance for *P. stewartii*, but may serve as a model for QS-systems in an array of other bacteria.

Appendix A

Trypsin BSA control experiment:

To address the question of whether or not the differential banding patterns in the presence and absence of AHL after trypsin digestion were on account of a conformational change in the protein opposed to altered protease activity, a control experiment was performed using BSA. BSA is not known to bind AHL, so it would be expected that the BSA conformation would remain constant in the presence and absence of AHL, resulting in conserved banding patterns after proteolysis.

BSA and HMGE (13.5 μM) were exposed to trypsin (53.6 nM) in the presence and absence of AHL (67.5 μM). Each condition had a final concentration of 1X trypsin buffer (20 mM $MgSO_4$, 20 mM Tris-HCl [pH 7.5], 10 mM $CaCl_2$. Reactions had a final volume of 50 μl.

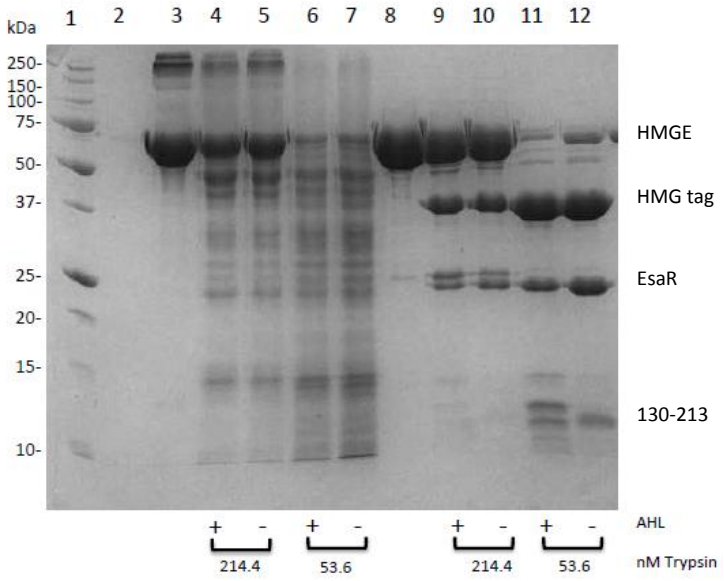

Impact of AHL on trypsin activity. BSA and HMGE were used at a final concentration of 13.5 µM. Samples were; 1, size standards; 2, trypsin; 3, BSA – AHL; 4, BSA + AHL + 214.4 nM trypsin; 5, BSA –AHL + 214.4 nM trypsin; 6, BSA + AHL + 53.6 nM trypsin; 7, BSA – AHL + 53.6 nM trypsin; 8, HMGE – AHL; 9, HMGE + AHL + 214.4 nM trypsin; 10, HMGE –AHL + 214.4 nM trypsin; 11, HMGE + AHL + 53.6 nM; 12, HMGE – AHL + 53.6 nM trypsin. Bands of interest indicated at the right side of the gel are reflective of lanes 8-12. The images are representative of experiments performed in duplicate.

References

1. **Alfano, J. R., and A. Collmer.** 2004. Type III secretion system effector proteins: double agents in bacterial disease and plant defense. Annu Rev Phytopathol **42:**385-414.
2. **Andersson, R. A., A. R. Eriksson, R. Heikinheimo, A. Mae, M. Pirhonen, V. Koiv, H. Hyytiainen, A. Tuikkala, and E. T. Palva.** 2000. Quorum sensing in the plant pathogen *Erwinia carotovora* subsp. *carotovora*: the role of *expR*(Ecc). Mol Plant Microbe Interact **13:**384-93.
3. **Andrews, S. C., D. Shipley, J. N. Keen, J. B. Findlay, P. M. Harrison, and J. R. Guest.** 1992. The haemoglobin-like protein (HMP) of *Escherichia coli* has ferrisiderophore reductase activity and its C-terminal domain shares homology with ferredoxin NADP+ reductases. FEBS Lett **302:**247-52.
4. **Beck von Bodman, S., and S. K. Farrand.** 1995. Capsular polysaccharide biosynthesis and pathogenicity in *Erwinia stewartii* require induction by an N-acylhomoserine lactone autoinducer. J Bacteriol **177:**5000-8.
5. **Bisi, D. C., and D. J. Lampe.** 2011. Secretion of Anti-Plasmodium Effector Proteins from a Natural *Pantoea agglomerans* Isolate by Using PelB and HlyA Secretion Signals. Appl Environ Microbiol **77:**4669-75.
6. **Bottomley, M. J., E. Muraglia, R. Bazzo, and A. Carfi.** 2007. Molecular insights into quorum sensing in the human pathogen *Pseudomonas aeruginosa* from the structure of the virulence regulator LasR bound to its autoinducer. J Biol Chem **282:**13592-600.
7. **Bradbury, J. F.** 1967. CMI Descriptions of Pathogenic Fungi and Bacteria.
8. **Braun, E.** 1982. Ultrastructural investigation of resistant and susceptible maize inbreds infected with *Erwinia stewartii*. Phytopathology **72:**159-166.
9. **Carlier, A. L., and S. B. von Bodman.** 2006. The *rcsA* Promoter of *Pantoea stewartii* subsp. *stewartii* Features a Low-Level Constitutive Promoter and an EsaR Quorum-Sensing-Regulated Promoter. J Bacteriol. **188:**4581-4584.
10. **Castang, S.** 2006. Direct Evidence for the Modulation of the Activity of the *Erwinia chrysanthemi* Quorum-sensing Regulator ExpR by Acylhomoserine Lactone Pheromone. J Biol Chem **281:**29972-29987.
11. **Chen, G., P. D. Jeffrey, C. Fuqua, Y. Shi, and L. Chen.** 2007. Structural basis for antiactivation in bacterial quorum sensing. Proc Natl Acad Sci U S A **104:**16474-9.
12. **Chen, G., L. R. Swem, D. L. Swem, D. L. Stauff, C. T. O'Loughlin, P. D. Jeffrey, B. L. Bassler, and F. M. Hughson.** 2011. A strategy for antagonizing quorum sensing. Mol Cell **42:**199-209.
13. **Chen, X., S. Schauder, N. Potier, A. Van Dorsselaer, I. Pelczer, B. L. Bassler, and F. M. Hughson.** 2002. Structural identification of a bacterial quorum-sensing signal containing boron. Nature **415:**545-9.
14. **Choi, S. H., and E. P. Greenberg.** 1991. The C-terminal region of the *Vibrio fischeri* LuxR protein contains an inducer-independent *lux* gene activating domain. Proc Natl Acad Sci U S A **88:**11115-9.
15. **Choi, S. H., and E. P. Greenberg.** 1992. Genetic dissection of DNA binding and luminescence gene activation by the *Vibrio fischeri* LuxR protein. J Bacteriol **174:**4064-9.
16. **Chung, J., E. Goo, S. Yu, O. Choi, J. Lee, J. Kim, H. Kim, J. Igarashi, H. Suga, J. S. Moon, I. Hwang, and S. Rhee.** 2011. Small-molecule inhibitor binding to an N-acyl-homoserine lactone synthase. Proc Natl Acad Sci U S A **108:**12089-94.

17. **Cook, K. A., R. A. Weinzierl, J. K. Pataky, P. D. Esker, and F. W. Nutter, Jr.** 2005. Population densities of corn flea beetle (Coleoptera: Chrysomelidae) and incidence of Stewart's wilt in sweet corn. J Econ Entomol **98:**673-82.
18. **Devine, J. H., G. S. Shadel, and T. O. Baldwin.** 1989. Identification of the operator of the *lux* regulon from the *Vibrio fischeri* strain ATCC7744. Proc Natl Acad Sci U S A **86:**5688-92.
19. **Dong, Y. H., A. R. Gusti, Q. Zhang, J. L. Xu, and L. H. Zhang.** 2002. Identification of quorum-quenching N-acyl homoserine lactonases from *Bacillus* species. Appl Environ Microbiol **68:**1754-9.
20. **Dunny, G. M., and B. A. Leonard.** 1997. Cell-cell communication in gram-positive bacteria. Annu Rev Microbiol **51:**527-64.
21. **Eberhard, A.** 1972. Inhibition and activation of bacterial luciferase synthesis. J Bacteriol **109:**1101-5.
22. **Eberhard, A., A. L. Burlingame, C. Eberhard, G. L. Kenyon, K. H. Nealson, and N. J. Oppenheimer.** 1981. Structural identification of autoinducer of *Photobacterium fischeri* luciferase. Biochemistry **20:**2444-9.
23. **Engebrecht, J., K. Nealson, and M. Silverman.** 1983. Bacterial bioluminescence: isolation and genetic analysis of functions from *Vibrio fischeri*. Cell **32:**773-81.
24. **Engebrecht, J., and M. Silverman.** 1984. Identification of genes and gene products necessary for bacterial bioluminescence. Proc Natl Acad Sci U S A **81:**4154-8.
25. **Ennis, H. L., D. N. Dao, S. U. Pukatzki, and R. H. Kessin.** 2000. *Dictyostelium amoebae* lacking an F-box protein form spores rather than stalk in chimeras with wild type. Proc Natl Acad Sci U S A **97:**3292-7.
26. **Finney, A. H., R. J. Blick, K. Murakami, A. Ishihama, and A. M. Stevens.** 2002. Role of the C-terminal domain of the alpha subunit of RNA polymerase in LuxR-dependent transcriptional activation of the *lux* operon during quorum sensing. J Bacteriol. **184:**4520-8.
27. **Flickinger, S. T., M. F. Copeland, E. M. Downes, A. T. Braasch, H. H. Tuson, Y. J. Eun, and D. B. Weibel.** 2011. Quorum Sensing between *Pseudomonas aeruginosa* Biofilms Accelerates Cell Growth. J Am Chem Soc **133:**5966-75.
28. **Frederix, M., A. Edwards, C. McAnulla, and J. A. Downie.** 2011. Co-ordination of quorum-sensing regulation in *Rhizobium leguminosarum* by induction of an anti-repressor. Mol Microbiol **81:**994-1007.
29. **Fuqua, C., and E. P. Greenberg.** 2002. Signalling: Listening in on bacteria: acyl-homoserine lactone signalling. Nature Reviews Molecular Cell Biology **3:**685-695.
30. **Fuqua, C., M. R. Parsek, and E. P. Greenberg.** 2001. Regulation of gene expression by cell-to-cell communication: acyl-homoserine lactone quorum sensing. Annu Rev Genet **35:**439-68.
31. **Gilson, L., A. Kuo, and P. V. Dunlap.** 1995. AinS and a new family of autoinducer synthesis proteins. J Bacteriol **177:**6946-51.
32. **Grant, S. G., J. Jessee, F. R. Bloom, and D. Hanahan.** 1990. Differential plasmid rescue from transgenic mouse DNAs into *Escherichia coli* methylation-restriction mutants. Proc Natl Acad Sci U S A **87:**4645-9.
33. **Gray, K. M., L. Passador, B. H. Iglewski, and E. P. Greenberg.** 1994. Interchangeability and specificity of components from the quorum-sensing regulatory systems of *Vibrio fischeri* and *Pseudomonas aeruginosa*. J Bacteriol **176:**3076-80.
34. **Hanahan, D.** 1983. Studies on transformation of *Escherichia coli* with plasmids. J Mol Biol **166:**557-80.
35. **Hanzelka, B. L., and E. P. Greenberg.** 1995. Evidence that the N-terminal region of the *Vibrio fischeri* LuxR protein constitutes an autoinducer-binding domain. J Bacteriol **177:**815-7.

36. **Herrera, C. M., M. D. Koutsoudis, X. Wang, and S. B. von Bodman.** 2008. *Pantoea stewartii* subsp. *stewartii* exhibits surface motility, which is a critical aspect of Stewart's wilt disease development on maize. Mol Plant Microbe Interact **21:**1359-70.
37. **Holden, M. T., S. Ram Chhabra, R. de Nys, P. Stead, N. J. Bainton, P. J. Hill, M. Manefield, N. Kumar, M. Labatte, D. England, S. Rice, M. Givskov, G. P. Salmond, G. S. Stewart, B. W. Bycroft, S. Kjelleberg, and P. Williams.** 1999. Quorum-sensing cross talk: isolation and chemical characterization of cyclic dipeptides from *Pseudomonas aeruginosa* and other gram-negative bacteria. Mol Microbiol **33:**1254-66.
38. **Hughes, D. T., and V. Sperandio.** 2008. Inter-kingdom signalling: communication between bacteria and their hosts. Nat Rev Microbiol **6:**111-20.
39. **Hwang, I., P. L. Li, L. Zhang, K. R. Piper, D. M. Cook, M. E. Tate, and S. K. Farrand.** 1994. TraI, a LuxI homologue, is responsible for production of conjugation factor, the Ti plasmid N-acylhomoserine lactone autoinducer. Proc Natl Acad Sci U S A **91:**4639-43.
40. **Johnson, D. C., A. Ishihama, and A. M. Stevens.** 2003. Involvement of region 4 of the sigma70 subunit of RNA polymerase in transcriptional activation of the *lux* operon during quorum sensing. FEMS Microbiol Lett **228:**193-201.
41. **Kempner, E. S., and F. E. Hanson.** 1968. Aspects of light production by *Photobacterium fischeri*. J Bacteriol **95:**975-9.
42. **Koziski, J. M.** 2008. Genetic analysis of the quorum-sensing regulator EsaR. Master's Thesis. Virginia Tech, Blacksburg.
43. **Leigh, J. A., and D. L. Coplin.** 1992. Exopolysaccharides in plant-bacterial interactions. Annu Rev Microbiol **46:**307-46.
44. **LiCata, V. J., and A. J. Wowor.** 2008. Applications of fluorescence anisotropy to the study of protein-DNA interactions. Methods Cell Biol **84:**243-62.
45. **Lintz, M. J., K. I. Oinuma, C. L. Wysoczynski, E. P. Greenberg, and M. E. Churchill.** 2011. Crystal structure of QscR, a *Pseudomonas aeruginosa* quorum sensing signal receptor. Proc Natl Acad Sci U S A.
46. **Loh, J., R. W. Carlson, W. S. York, and G. Stacey.** 2002. Bradyoxetin, a unique chemical signal involved in symbiotic gene regulation. Proc Natl Acad Sci U S A **99:**14446-51.
47. **Luo, Z. Q., Y. Qin, and S. K. Farrand.** 2000. The antiactivator TraM interferes with the autoinducer-dependent binding of TraR to DNA by interacting with the C-terminal region of the quorum-sensing activator. J Biol Chem **275:**7713-22.
48. **Majdalani, N., and S. Gottesman.** 2005. The Rcs phosphorelay: a complex signal transduction system. Annu Rev Microbiol **59:**379-405.
49. **Majdalani, N., M. Heck, V. Stout, and S. Gottesman.** 2005. Role of RcsF in signaling to the Rcs phosphorelay pathway in *Escherichia coli*. J Bacteriol **187:**6770-8.
50. **Meighen, E. A.** 1991. Molecular biology of bacterial bioluminescence. Microbiol Rev **55:**123-42.
51. **Mergaert, J., L. Verdonck, and K. Kersters.** 1993. Transfer of *Erwinia ananas* (synonym, *Erwinia uredovora*) and *Erwinia stewartii* to the Genus *Pantoea* emend. as *Pantoea ananas* (Serrano 1928) comb. nov. and *Pantoea stewartii* (Smith 1898) comb. nov., Respectively, and Description of *Pantoea stewartii* subsp. *indologenes* subsp. nov. Int J Syst Bacteriol **43:**162-173.
52. **Minogue, T. D., A. L. Carlier, M. D. Koutsoudis, and S. B. von Bodman.** 2005. The cell density-dependent expression of stewartan exopolysaccharide in *Pantoea stewartii* ssp. *stewartii* is a function of EsaR-mediated repression of the *rcsA* gene. Mol Microbiol **56:**189-203.
53. **Minogue, T. D., M. Wehland-von Trebra, F. Bernhard, and S. B. von Bodman.** 2002. The autoregulatory role of EsaR, a quorum-sensing regulator in *Pantoea stewartii* ssp. *stewartii*: evidence for a repressor function. Mol Microbiol **44:**1625-35.

54. **Morohoshi, T., Y. Nakamura, G. Yamazaki, A. Ishida, N. Kato, and T. Ikeda.** 2007. The plant pathogen *Pantoea ananatis* produces N-acylhomoserine lactone and causes center rot disease of onion by quorum sensing. J Bacteriol **189:**8333-8.
55. **Nallamsetty, S., B. P. Austin, K. J. Penrose, and D. S. Waugh.** 2005. Gateway vectors for the production of combinatorially-tagged His6-MBP fusion proteins in the cytoplasm and periplasm of *Escherichia coli*. Protein Sci **14:**2964-71.
56. **Nasser, W., M. L. Bouillant, G. Salmond, and S. Reverchon.** 1998. Characterization of the *Erwinia chrysanthemi expI-expR* locus directing the synthesis of two N-acyl-homoserine lactone signal molecules. Mol Microbiol **29:**1391-405.
57. **Nealson, K. H., T. Platt, and J. W. Hastings.** 1970. Cellular control of the synthesis and activity of the bacterial luminescent system. J Bacteriol **104:**313-22.
58. **Ng, W. L., and B. L. Bassler.** 2009. Bacterial quorum-sensing network architectures. Annu Rev Genet **43:**197-222.
59. **Nimtz, M., A. Mort, V. Wray, T. Domke, Y. Zhang, D. L. Coplin, and K. Geider.** 1996. Structure of stewartan, the capsular exopolysaccharide from the corn pathogen *Erwinia stewartii*. Carbohydr Res **288:**189-201.
60. **Pappas, K. M., C. L. Weingart, and S. C. Winans.** 2004. Chemical communication in proteobacteria: biochemical and structural studies of signal synthases and receptors required for intercellular signalling. Molecular Microbiology **53:**755-769.
61. **Pesci, E. C., J. P. Pearson, P. C. Seed, and B. H. Iglewski.** 1997. Regulation of *las* and *rhl* quorum sensing in *Pseudomonas aeruginosa*. J Bacteriol **179:**3127-32.
62. **Pompeani, A. J., J. J. Irgon, M. F. Berger, M. L. Bulyk, N. S. Wingreen, and B. L. Bassler.** 2008. The *Vibrio harveyi* master quorum-sensing regulator, LuxR, a TetR-type protein is both an activator and a repressor: DNA recognition and binding specificity at target promoters. Mol Microbiol **70:**76-88.
63. **Roper, M. C.** 2011. *Pantoea stewartii* subsp. *stewartii*: lessons learned from a xylem-dwelling pathogen of sweet corn. Mol Plant Pathol.
64. **Ruby, E. G.** 1996. Lessons from a cooperative, bacterial-animal association: the *Vibrio fischeri-Euprymna scolopes* light organ symbiosis. Annu Rev Microbiol **50:**591-624.
65. **Sandoz, K. M., S. M. Mitzimberg, and M. Schuster.** 2007. Social cheating in *Pseudomonas aeruginosa* quorum sensing. Proc Natl Acad Sci U S A **104:**15876-81.
66. **Schaefer, A. L., E. P. Greenberg, C. M. Oliver, Y. Oda, J. J. Huang, G. Bittan-Banin, C. M. Peres, S. Schmidt, K. Juhaszova, J. R. Sufrin, and C. S. Harwood.** 2008. A new class of homoserine lactone quorum-sensing signals. Nature **454:**595-599.
67. **Schaefer, A. L., D. L. Val, B. L. Hanzelka, J. E. Cronan, Jr., and E. P. Greenberg.** 1996. Generation of cell-to-cell signals in quorum sensing: acyl homoserine lactone synthase activity of a purified *Vibrio fischeri* LuxI protein. Proc Natl Acad Sci U S A **93:**9505-9.
68. **Schu, D. J.** 2009. Structure/Function Analysis of the Quorum-Sensing Regulator EsaR from the Plant Pathogen *Pantoea stewartii*. Ph.D. Thesis. Virginia Tech, Blacksburg.
69. **Schu, D. J., A. L. Carlier, K. P. Jamison, S. von Bodman, and A. M. Stevens.** 2009. Structure/Function Analysis of the *Pantoea stewartii* Quorum-Sensing Regulator EsaR as an Activator of Transcription. J Bacteriol **191:**7402-7409.
70. **Schu, D. J., R. Ramachandran, J. S. Geissinger, and A. M. Stevens.** 2011. Probing the impact of ligand binding on the acyl-homoserine lactone-hindered transcription factor EsaR of *Pantoea stewartii* subsp. *stewartii*. J Bacteriol.
71. **Seet, Q., and L. H. Zhang.** 2011. Anti-activator QslA defines the quorum sensing threshold and response in *Pseudomonas aeruginosa*. Mol Microbiol **80:**951-65.

72. **Shadel, G. S., and T. O. Baldwin.** 1991. The *Vibrio fischeri* LuxR protein is capable of bidirectional stimulation of transcription and both positive and negative regulation of the *luxR* gene. J Bacteriol **173:**568-74.
73. **Stevens, A. M., N. Fujita, A. Ishihama, and E. P. Greenberg.** 1999. Involvement of the RNA polymerase alpha-subunit C-terminal domain in LuxR-dependent activation of the *Vibrio fischeri* luminescence genes. J Bacteriol **181:**4704-7.
74. **Stevens, A. M., Queneau, Y., Soulere, L., von Bodman, S., Doutheau, A.** 2011. Mechanisms and Synthetic Modulators of AHL-Dependent Gene Regulation. Chemical Reviews **In Press**.
75. **Thomas, P. W., and W. Fast.** 2011. Heterologous overexpression, purification, and in vitro characterization of AHL lactonases. Methods Mol Biol **692:**275-90.
76. **Thomson, N. R., M. A. Crow, S. J. McGowan, A. Cox, and G. P. Salmond.** 2000. Biosynthesis of carbapenem antibiotic and prodigiosin pigment in *Serratia* is under quorum sensing control. Mol Microbiol **36:**539-56.
77. **Torres-Cabassa, A., S. Gottesman, R. D. Frederick, P. J. Dolph, and D. L. Coplin.** 1987. Control of extracellular polysaccharide synthesis in *Erwinia stewartii* and *Escherichia coli* K-12: a common regulatory function. J Bacteriol **169:**4525-31.
78. **Trott, A. E., and A. M. Stevens.** 2001. Amino acid residues in LuxR critical for its mechanism of transcriptional activation during quorum sensing in *Vibrio fischeri*. J Bacteriol **183:**387-92.
79. **Tsai, C. S., and S. C. Winans.** 2010. LuxR-type quorum-sensing regulators that are detached from common scents. Mol Microbiol **77:**1072-82.
80. **Tsai, C. S., and S. C. Winans.** 2011. The quorum-hindered transcription factor YenR of *Yersinia enterocolitica* inhibits pheromone production and promotes motility via a small non-coding RNA. Mol Microbiol **80:**556-71.
81. **Urbanowski, M. L., C. P. Lostroh, and E. P. Greenberg.** 2004. Reversible acyl-homoserine lactone binding to purified *Vibrio fischeri* LuxR protein. J Bacteriol **186:**631-7.
82. **Vannini, A., C. Volpari, C. Gargioli, E. Muraglia, R. Cortese, R. De Francesco, P. Neddermann, and S. D. Marco.** 2002. The crystal structure of the quorum sensing protein TraR bound to its autoinducer and target DNA. EMBO J **21:**4393-401.
83. **Vannini, A., C. Volpari, C. Gargioli, E. Muraglia, R. De Francesco, P. Neddermann, and S. Di Marco.** 2002. Crystallization and preliminary X-ray diffraction studies of the transcriptional regulator TraR bound to its cofactor and to a specific DNA sequence. Acta Crystallogr D Biol Crystallogr **58:**1362-4.
84. **Velicer, G. J., L. Kroos, and R. E. Lenski.** 2000. Developmental cheating in the social bacterium *Myxococcus xanthus*. Nature **404:**598-601.
85. **von Bodman, S. B., J. K. Ball, M. A. Faini, C. M. Herrera, T. D. Minogue, M. L. Urbanowski, and A. M. Stevens.** 2003. The quorum sensing negative regulators EsaR and ExpR(Ecc), homologues within the LuxR family, retain the ability to function as activators of transcription. J Bacteriol **185:**7001-7.
86. **von Bodman, S. B., D. R. Majerczak, and D. L. Coplin.** 1998. A negative regulator mediates quorum-sensing control of exopolysaccharide production in *Pantoea stewartii* subsp. *stewartii*. Proc Natl Acad Sci U S A **95:**7687-92.
87. **von Bodman, S. B., J. M. Willey, and S. P. Diggle.** 2008. Cell-cell communication in bacteria: united we stand. J Bacteriol **190:**4377-91.
88. **Waters, C. M., and B. L. Bassler.** 2005. Quorum sensing: cell-to-cell communication in bacteria. Annu Rev Cell Dev Biol **21:**319-46.
89. **Wei, S. L., and R. E. Young.** 1989. Development of symbiotic bacterial bioluminescence in a nearshore cephalopod, *Euprymna scolopes*. Marine Biology **103:**541-546.

90. **Welch, M., D. E. Todd, N. A. Whitehead, S. J. McGowan, B. W. Bycroft, and G. P. Salmond.** 2000. N-acyl homoserine lactone binding to the CarR receptor determines quorum-sensing specificity in *Erwinia*. EMBO J **19:**631-41.
91. **Whitehead, N. A., A. M. Barnard, H. Slater, N. J. Simpson, and G. P. Salmond.** 2001. Quorum-sensing in Gram-negative bacteria. FEMS Microbiol Rev **25:**365-404.
92. **Williams, J. W., X. Cui, A. Levchenko, and A. M. Stevens.** 2008. Robust and sensitive control of a quorum-sensing circuit by two interlocked feedback loops. Mol Syst Biol **4:**234.
93. **Yang, Y., and V. J. LiCata.** 2011. Interactions of replication versus repair DNA substrates with the Pol I DNA polymerases from *Escherichia coli* and *Thermus aquaticus*. Biophys Chem **159:**188-93.
94. **Yao, Y., M. A. Martinez-Yamout, T. J. Dickerson, A. P. Brogan, P. E. Wright, and H. J. Dyson.** 2006. Structure of the *Escherichia coli* quorum sensing protein SdiA: activation of the folding switch by acyl homoserine lactones. J Mol Biol **355:**262-73.
95. **You, L., R. S. Cox, 3rd, R. Weiss, and F. H. Arnold.** 2004. Programmed population control by cell-cell communication and regulated killing. Nature **428:**868-71.
96. **Zhang, R. G., T. Pappas, J. L. Brace, P. C. Miller, T. Oulmassov, J. M. Molyneaux, J. C. Anderson, J. K. Bashkin, S. C. Winans, and A. Joachimiak.** 2002. Structure of a bacterial quorum-sensing transcription factor complexed with pheromone and DNA. Nature **417:**971-4.
97. **Zhang, Y. Z., G. Wang, H. Q. Hu, S. H. Wei, J. Ji, J. J. Wang, and C. Li.** 2002. Transfer of insecticidal protein gene from *Bacillus thuringiensis* into conventional maize inbred-line mediated by *Agrobacterium tumefaciens*. Yi Chuan **24:**35-9.
98. **Zheng, H., Z. Zhong, X. Lai, W. X. Chen, S. Li, and J. Zhu.** 2006. A LuxR/LuxI-type quorum-sensing system in a plant bacterium, *Mesorhizobium tianshanense*, controls symbiotic nodulation. J Bacteriol **188:**1943-9.
99. **Zhu, J., and S. C. Winans.** 1999. Autoinducer binding by the quorum-sensing regulator TraR increases affinity for target promoters in vitro and decreases TraR turnover rates in whole cells. Proc Natl Acad Sci U S A **96:**4832-7.
100. **Zhu, J., and S. C. Winans.** 2001. The quorum-sensing transcriptional regulator TraR requires its cognate signaling ligand for protein folding, protease resistance, and dimerization. Proc Natl Acad Sci U S A **98:**1507-12.